NOAA Technical Memorandum NMFS

File Copy

#2

SEPTEMBER 2002

MONTHLY MEAN COASTAL UPWELLING INDICES, WEST COAST OF SOUTH AFRICA 1981 TO 2000: TRENDS AND RELATIONSHIPS

Jerrold G. Norton

Frank B. Schwing

Mark H. Pickett

Steven G. Cummings

David M. Husby

Phaedra Green Jessen

NOAA-TM-NMFS-SWFSC-343

U.S. DEPARTMENT OF COMMERCE
National Oceanic and Atmospheric Administration
National Marine Fisheries Service
Southwest Fisheries Science Center

The National Oceanic and Atmospheric Administration (NOAA), organized in 1970, has evolved into an agency which establishes national policies and manages and conserves our oceanic, coastal, and atmospheric resources. An organizational element within NOAA, the Office of Fisheries is responsible for fisheries policy and the direction of the National Marine Fisheries Service (NMFS).

In addition to its formal publications, the NMFS uses the NOAA Technical Memorandum series to issue informal scientific and technical publications when complete formal review and editorial processing are not appropriate or feasible. Documents within this series, however, reflect sound professional work and may be referenced in the formal scientific and technical literature.

NOAA Technical Memorandum NMFS
This TM series is used for documentation and timely communication of preliminary results, interim reports, or special purpose information. The TMs have not received complete formal review, editorial control, or detailed editing.

SEPTEMBER 2002

MONTHLY MEAN COASTAL UPWELLING INDICES, WEST COAST OF SOUTH AFRICA 1981 TO 2000: TRENDS AND RELATIONSHIPS

Jerrold G. Norton[1], Frank B. Schwing[1], Mark H. Pickett[1],
Steven G. Cummings[1], David M. Husby[1,2], Phaedra Green Jessen[1,2]

[1]Pacific Fisheries Environmental Laboratory
Southwest Fisheries Science Center
1352 Lighthouse Ave., Pacific Grove, CA, 93950

[2]Joint Institute for Marine and Atmospheric Research (JIMAR)
University of Hawaii at Manoa
1000 Pope Road, Honolulu, HI, 96822

NOAA-TM-NMFS-SWFSC-343

U.S. DEPARTMENT OF COMMERCE
Donald L. Evans, Secretary
National Oceanic and Atmospheric Administration
VADM Conrad C. Lautenbacher, Jr., Undersecretary for Oceans and Atmosphere
National Marine Fisheries Service
William T. Hogarth, Assistant Administrator for Fisheries

CONTENTS

FIGURES AND TABLES:

ABSTRACT

The Pacific Fisheries Environmental Laboratory (PFEL) Upwelling Index provides continuous proxy time series of coastal ocean processes which are difficult to measure directly and are infrequently available as multiyear time series for the study of surface layer physical and biological ocean dynamics. The PFEL Upwelling Index (UI) is derived from analyzed pressure fields using planetary boundary layer theory and geostrophic wind approximation to derive inferences about momentum transport from the wind to the sea surface layer. The UI values for the period January 1981 through December 2000 are presented for the highly productive upwelling systems off the coast of southwest Africa. These data have been extracted for three sets of nine locations from 15° to 36°S. Large-scale characteristics of these time series include: 1) Highest UI values are in the austral spring and summer; 2) Maximum UI occurs earlier in the year at lower latitudes; 3) South of 33° S, mean UI is negative for short periods during austral winter; 4) Interannual variation is greatest in the north, but south of 33°S there is also a maximum in standard deviation during austral winter; 5) Austral spring and summer UI increases from 36° to 27°S; 6) Variation in UI is dependent on computation point, distance from shore and adjacent land topography; and 7) Radiative atmospheric heating over adjacent desert may enhance UI from 21°S equatorward. The UI for the west coast of southern Africa reflects physical environmental changes expected to influence temporally and spatially coincident ecosystems by indicating nutrient availability in the euphotic zone.

INTRODUCTION

Since the early 1970's, the Pacific Fisheries Environmental Laboratory (PFEL) has produced indices of offshore Ekman transport, or upwelling indices, along the west coast of North America (Bakun, 1973). These indices are calculated from surface atmospheric pressure fields produced by the U. S. Navy Fleet Numerical Meteorology and Oceanography Center (Clancy, 1992; Rosmond, 1992). Subsequent development by Bakun (1975), Mason and Bakun (1986), and Schwing et al. (1996) allows the PFEL Upwelling Index (UI) and associated atmospheric parameters (*APPENDIX II*) to be calculated for any location in the world's oceans. These products are regularly distributed to users worldwide, including scientific researchers, resource managers, private entrepreneurs and sportsmen.

The frictional stress of equatorward wind on the ocean balanced with the Coriolis force causes water in the surface layer to move away from the west coast of Africa (Sverdrup et al., 1942; Wooster and Reid, 1963; Smith, 1968; Bakun, 1975; Parrish et al., 1983). The offshore moving surface water, referred to as Ekman transport, is replaced by water which upwells to the surface layer of the coastal ocean from depths of 10 to more than 60 meters, depending on vertical patterns of ocean stability (Figure 1).

Upwelled water is typically cooler than the surface water displaced offshore and frequently has greater dissolved nutrient concentrations if the upwelled water is from below the euphotic zone (Wooster and Reid, 1963; Smith, 1968; Thomas et al., 1994; Strub et al., 1998b). These

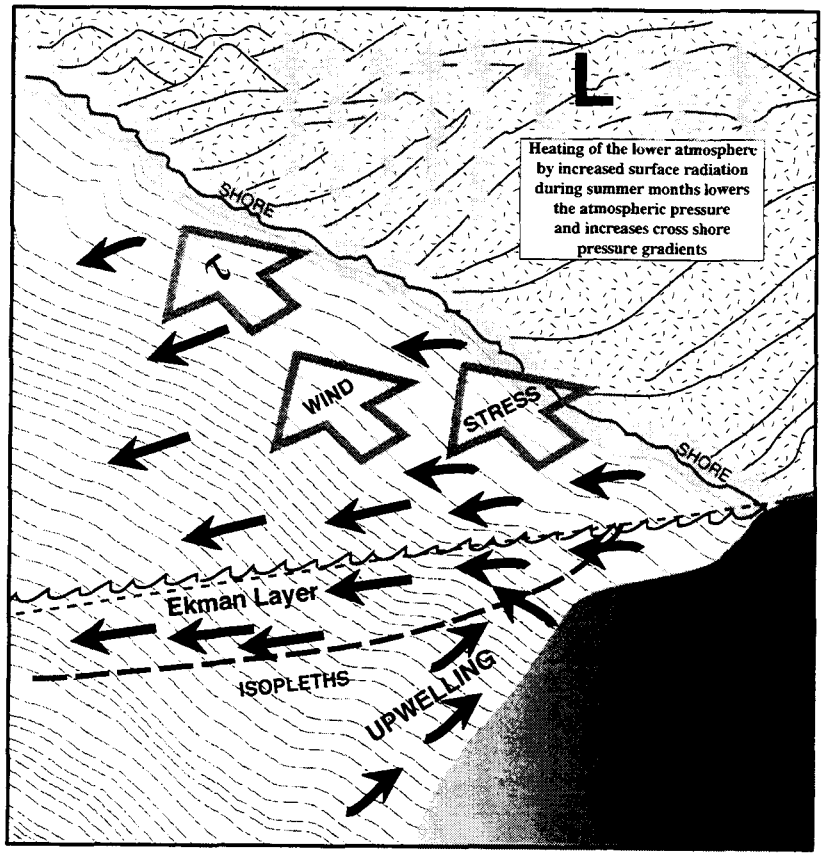

Figure 1. Diagram of the effects of winds stress (open arrows) on coastal upwelling and offshore Ekman transport (black arrows) along the southwest coast of Africa. Mean winds blow from south to north enhancing coastal upwelling of subsurface water. Upwelling leads to an onshore-offshore pressure gradient, with lower sea level shoreward compared to a level surface (smaller dashed line). Gray, wavy, vertical arrows suggest surface heating over land leading to low pressure typical of the austral summer. Equatorward wind stress occurs at the eastern limb of the south Atlantic subtropical high atmospheric pressure system.

nutrients are essential in sustaining primary production and higher trophic levels (Peterson and Miller, 1977; Traganza et al., 1981; Thomas et al., 1994). For this reason, upwelling ecosystems are highly productive (Wooster and Reid, 1963; Ryther, 1969). Primary production commonly exceeds 2 g carbon per m^2 per day in each of the major upwelling regions. Fish production within the eastern Pacific and eastern Atlantic upwelling regions each may exceed a million metric tons per year (Mann and Lazier, 1996). Upwelling indices have been correlated with condition factors, recruitment and abundance of commercially important fish throughout the world (Ryther, 1969; Parrish et al., 1981; Norton, 1987; Cury et al., 1995; Ainley et al., 1994; Thomas et al., 1994; VenTresca et al., 1995; Durand et al., 1998).

Currently PFEL generates synoptic scale (100 to 1000 km) wind and ocean transport indices (*APPENDIX II*) which include the UI for Peru-Chile and California Current upwelling ecosystems. This study was done in accordance with the goals of PFEL to provide an expanding body of meaningful physical environmental data to the fisheries research and management communities.

Upwelling Index computations have been made from U. S. Navy Fleet Numerical Meteorology and Oceanography Center (FNMOC) monthly mean pressure fields for 24 locations in the Benguela Current upwelling system along the west coast of South Africa. Seven computation locations are within 100 km of the local coastline. Ten locations are more than 100 km offshore and there are seven additional Cross Shore locations (Figure 2). These locations were chosen to illustrate the effects of the continental boundary and the Namibian coastal desert on UI computations.

The Benguela Current is bordered by land of generally low relief. Few peaks exceed 1500 m in the 300 km-wide coastal strip from 15° S to 30° S. North of 30° S, the Namibian Desert extends from the coast up to 100 km inland where it gives way to hills of low relief which extend well into the west African interior. The Kalahari Desert is about 500 km inland at 25° S. South of 30° S, the Cape Columbine area is also of low relief, but mountains north of Cape Agulhas and Cape of Good Hope exceed 2,000 meters height.

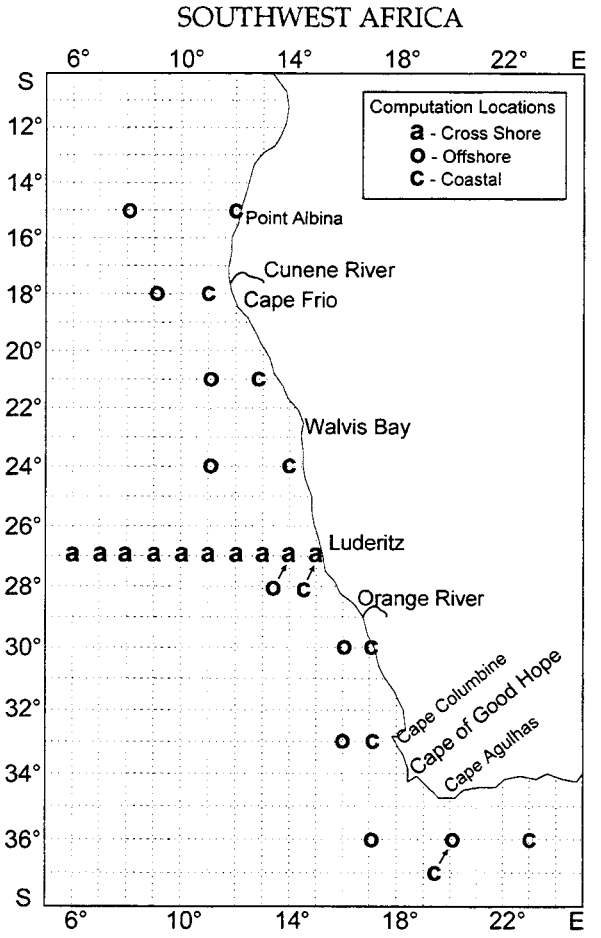

Figure 2. Upwelling Index (UI) computation locations off the southwest coast of Africa. These computation locations represent both nearshore (Coastal), within 100 km of shore, and oceanic (Offshore, Cross Shore) environments.

As in other eastern boundary current systems, wind forced coastal and ocean divergence, or upwelling, in the Benguela Current region brings supplies of nutrients into the euphotic zone, which in turn promote abundant primary production. Waldron and Probyn (1992) estimate the annual new production in the Benguela Current system to be 4.7 x 10^{13} g C yr^{-1}. This value is 0.6-1.4% of the total new production estimated for all the world's oceans. Since the Benguela region is only 0.02% of the world's ocean, the comparison suggests that the Benguela region provides the environment for greater than 30 times more productivity per km^2 than the average productivity of the world's ocean (Mann and Lazier, 1996).

Coastal Zone Color Scanner (CZCS) composite images for the 1978 to 1986 period (Longhurst, 1998) show a 100 to 300 km-wide band of high chlorophyll (1-5 mg Chl m^3) water extending along the coast from the area of Cape Columbine (35°S) to north of Point Albina (15°S). A large portion of the high primary productivity is due to local and remote wind-forced upwelling of nutrients into the euphotic zone (e.g. Figure 1) (Wooster and Reid, 1963; Gill, 1982). Three areas of especially intense or persistent upwelling have been identified near Luderitz, near Cape Frio, and in the Cape of Good Hope area (Figure 2). In the CZCS imagery, the Luderitz area has a wider band of high productivity in the austral summer and the Cape Frio area has a wider band in austral fall and winter (Longhurst, 1998). Annual export of photosynthetic carbon (Waldron and Probyn 1992) may be greater from the Cape Frio area (Falkowski, et al., 1998). Local UI variability and geographical setting are also important in determining the location of greatest new carbon compound production.

In comparing two years of Geosat altimeter and Advanced Very High Resolution Radiometer (AVHRR) Sea Surface Temperature (SST) data, Strub et al. (1998) found that upwelling in the Cape of Good Hope Region (32–34°S) is more seasonal than at Luderitz, but more complicated in circulation because of the energetic eddy field of the Agulhas retroflection and the subtropical convergence zone. Circulation in the Cape Frio region is complicated by southward excursions of the Angola front (Cole and McGlade, 1997). North of 32°S the winds are upwelling favorable throughout the year (Parrish et al., 1983; Bakun and Nelson, 1991; Strub et al., 1998).

A 35-year record of upwelling at Cape Columbine (32.8°S), computed from measured winds, shows a distinct annual cycle of two to three times the annual mean (Johnson and Nelson, 1999). When seasonal trends are removed with a 13 point summation filter, two-fold fluctuations lasting three to seven years are evident in the filtered series. Over the 1980 to 1992 interval, computed upwelling fell to less than 40% of the 1980 record high, remained low until late 1989, rose through 1990 to about 60% of the 1980 high and remained at this level through 1992. The apparent shift in 1990 to increased upwelling, observed by Johnson and Nelson (1999), is also seen in the UI computations presented below.

Since 1984, South African pelagic stocks of anchovy, *Engraulis capensis*, and sardine, *Sardinops sagax*, have been monitored acoustically as an aid in managing harvest. It appears that changes have occurred in the ecosystem, favoring sardines over anchovy, during the 1984 to 1999 period (Schwartzlose et al., 1999). Since these fish integrate the environment on time scales of 1-4 years, changes in species abundance may be related to the shifts in the oceanic environment indicated by the Cape Columbine upwelling record. Sardine spawner biomass has increased from 100,000 tons in the 1984 to 1988 period to more than 500,000 tons in the 1994 to 1999 period. At the same time, anchovy spawner biomass has dropped from more than 1,000,000 tons in the 1984 to 1988 period to less than 500,000 tons in the 1994 to 1999 period (Schwartzlose et al., 1999). Seabird diet also reflects these changes in relative abundance of anchovy and sardine (Crawford, 1998).

COMPUTATIONS AND ANALYSES

PFEL UI calculations are based on Ekman's (1905) theoretical derivations of steady mass transport due to the momentum balance between Coriolis acceleration acting on the current and the divergence of the wind stress, assuming homogeneity, uniform wind, and steady state conditions. The mass transport of surface water due to wind stress is 90° to the left (right) of the wind when the wind is pressing on an observer's back in the southern (northern) hemisphere.

The depth to which an appreciable amount of offshore transport occurs is termed the Surface Ekman Layer which is generally 20 to 30 m deep (Figure 1), but can be more than 60 m deep depending on surface wind speed, wind direction, and ocean stratification (Lentz, 1992; Price and Sundermeyer, 1999). Upwelling of temperature, salinity, nutrient and density isopleths may be observed below 300 m depth, but the water brought into the euphotic zone is seldom from these depths.

Global gridded sea level atmospheric pressure fields became available from Fleet Numerical Meteorology and Oceanography Center (FNMOC) in 1981. These 2.5° x 2.5° (73 x 144 global spherical projection) grids are produced at six hour intervals from incoming observations, forecasts and analyses (Clancy, 1992; Rosmond, 1992). UI calculations were

made after extrapolating the 2.5° x 2.5° pressure fields to a 3° computation grid length on a spherical coordinate system using a Bessel 16-point central difference formula. This maintains the 3° x 3° (Figure 3, solid shading) conventions used in previous UI calculations (Bakun, 1973; Bakun, 1975). In November 1996, the 2.5° x 2.5° fields were replaced with 1° x 1° (360 x 181 global spherical projection) grids. Computations of UI for November 1996 to December 2000 are based on these more finely gridded data.

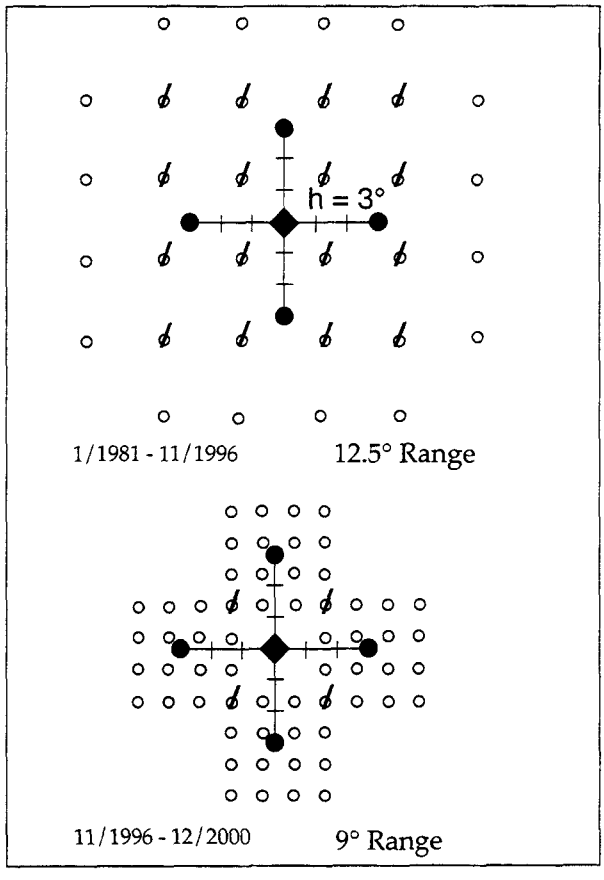

Figure 3. For all Upwelling Index (UI) computations, the specified point is the center square of the solid shaded 6° x 6° array. The solid shaded circles show derived points that are used to compute upwelling index at the central location. Derived computation points are computed from the 16 closest data grid points (open circles). The upper panel shows the range of grid points from which the computation points are calculated when the source global data grid has 2.5° x 2.5° length. The lower panel shows grid spacing for the 1° x 1° data grid currently used. Diagonals mark data grid points that are used more than once in the overall computation.

However, upwelling indices continue to be calculated from a 3° computational mesh wherein each point contributing to the final computation is derived from Bessel interpolation of the 16-point grid of the monthly mean sea level pressure field (Figure 3). This convention provides continuity through the 20-year data set presented.

In comparing mean sea level atmospheric pressure from the 1° x 1° fields to mean sea level atmospheric pressure from the 2.5° x 2.5° fields, it was found that the mean fields were nearly identical and generally agree to within tenths of a millibar (Schwing et al., 1996). However, differences are expected in the UI, because computations from the 2.5° x 2.5° fields smooth the physical gradients more than computations from the 1° x 1° fields (Figure 3).

For this report, monthly mean upwelling indices have been produced for 24 locations from 15°S to 36°S at 20 to 900 km from shore (Figure 2). This range extends from tropical to temperate climates. The UI computation, reviewed below, follows the procedures used in all previous PFEL UI computations (Bakun, 1973, 1975; Mason and Bakun, 1986; Schwing et al., 1996; Norton et al., 2001).

Derivatives of the sea level atmospheric pressure, **P**, at each computation point are estimated by taking the difference in pressure between the grid points to either side and dividing by the 6° angular grid length (Figure 3, solid shading, center).

$$\partial P/\partial \phi \approx (P_{\lambda,\phi+h} - P_{\lambda,\phi-h})(2h)^{-1}; \qquad (1)$$

$$\partial P/\partial \lambda \approx (P_{\lambda+h,\phi} - P_{\lambda-h,\phi})(2h)^{-1}; \qquad (2)$$

where ϕ and λ are the north and east angular coordinates respectively, and **h** is the 3° mesh length in radians (Figure 3).

The east (u_g) and north (v_g) components of the geostrophic wind are:

$$u_g = -(f\rho_a R)^{-1} \partial P/\partial \phi; \qquad (3)$$

$$v_g = (f\rho_a R \cos \phi)^{-1} \partial P/\partial \lambda; \qquad (4)$$

where f is the Coriolis parameter (negative for Southern Hemisphere), ρ_a is the density of air (assumed constant at 1.22 kg/m^3), and **R** is the mean radius of the Earth (6,371.2 km).

Assuming no friction, the geostrophic wind is parallel to local isobars, with low pressure to the right in the Southern Hemisphere; specifically wind circulates clockwise (cyclonically) around Southern Hemisphere areas of low atmospheric pressure. To approximate frictional effects, equivalent sea surface wind vectors are estimated by rotating the geostrophic wind 15° to the right and reducing its magnitude by 30%.

Sea surface wind stress is calculated from the geostrophic wind using the square-law formula:

$$\vec{\tau} = \rho_a C_d |\vec{v}| \vec{v} \; ; \qquad (5)$$

where $\vec{\tau}$ is the wind stress vector, C_d is an empirical drag coefficient, and

$\vec{v}$ is the estimated wind vector near the sea surface with magnitude $|v|$. The value used to calculate upwelling from the monthly-mean fields is C_d = 0.0026 (Bakun, 1973; Davidson, 1974; Nelson, 1977, Thompson, et al., 1983). A C_d = 0.0013 was used by Bakun (1975) for the calculation of UI from six-hourly FNMOC pressure fields.

Ekman transport, $\vec{M}$, is calculated using:

$$\vec{M} = (\vec{\tau} \times \vec{k}) f^{-1} \; ; \qquad (6)$$

where $\vec{k}$ is the unit vector directed vertically upward. The sign of the offshore component of Ekman transport, $M_x = \tau_y / f$, where **x** is normal and **y** parallel to the local coastline orientation, is reversed to reflect that negative (offshore) Ekman transport leads to positive vertical transport (upwelling). UI values are expressed in units of metric tons (cubic meters) per second per 100 meters of coastline (t/s/100m).

The UI is most generally interpreted as an index of upwelling occurring along 100-500 km of coastline, rather than an indicator of upwelling at the exact computation points. There is frequently considerable correlation between points computed at 3° intervals along the coast (see *RESULTS*).

Time series for each of the nine Benguela Current Offshore locations were fit to annual and semiannual sinusoids by least squares techniques (Lynn, 1967). These biharmonic fits, and an envelope of ±1.0 standard error (Schwing et al., 1996), are presented in graphical and tabular form. Biharmonic analysis fits the UI for time interval, **t**, at a particular computation point to equations of the form

$$UI(t) = A_0 + A_1\cos(2\Pi t) + B_1\sin(2\Pi t) + A_2\cos(4\Pi t) + B_2\sin(4\Pi t) \qquad (7)$$

where A_0 is the mean and A_n and B_n are coefficients that determine phase and amplitude of the fitted **n**th harmonic. The information given by biharmonic analysis will depend on how well the data are fit by the annual and semiannual harmonics. There will be an annual harmonic, unless there is no variation in the input data. If the input data do not form a perfectly symmetrical annual sinusoid, then there will be a semi-annual harmonic. However the amplitude of each harmonic will give an indication of the fit of the data to the hypothesized harmonic and the correlation coefficient (**r**) will give an indication of the overall fit.

RESULTS

Mean annual cycles of UI for the Offshore and Cross Shore computation points (Figure 4) are in qualitative agreement with accepted climatologies for the Benguela Current region (Parrish et al., 1983; Bakun and Nelson, 1991; Hill et al., 1998; Strub et al., 1998b).

North of 30°S upwelling may be continuous throughout the year (Figure 4), consistent with the European Center for Medium-Range Weather Forecasts (ECMWF) annual cycles presented by Hill et al. (1998). For the Offshore computation points (Figure 2), seasonal maximum in UI is most persistent at 27°S and occurs October through February (austral spring and summer). At 18° and 21° S the largest UI occurs in spring and decreases in summer (Figure 4, left panel). This pattern is consistent with the wind stress calculations of Parrish, et al. (1983) and Bakun and Nelson (1991). North of 24°S, seasonal excursions of UI are attenuated Offshore in more tropical annual patterns (Figure 5), but onshore, in both Coastal and Cross Shore computation sets, the annual cycle is extreme due to the increased summer heating of the atmosphere over the Namibian and inland deserts. PFEL UI computations closer than 300 km to the coast will have the eastern computation point (solid shading in Figure 3) on land; consequently, the low pressure system will be important in the computation of ocean Ekman transport (UI).

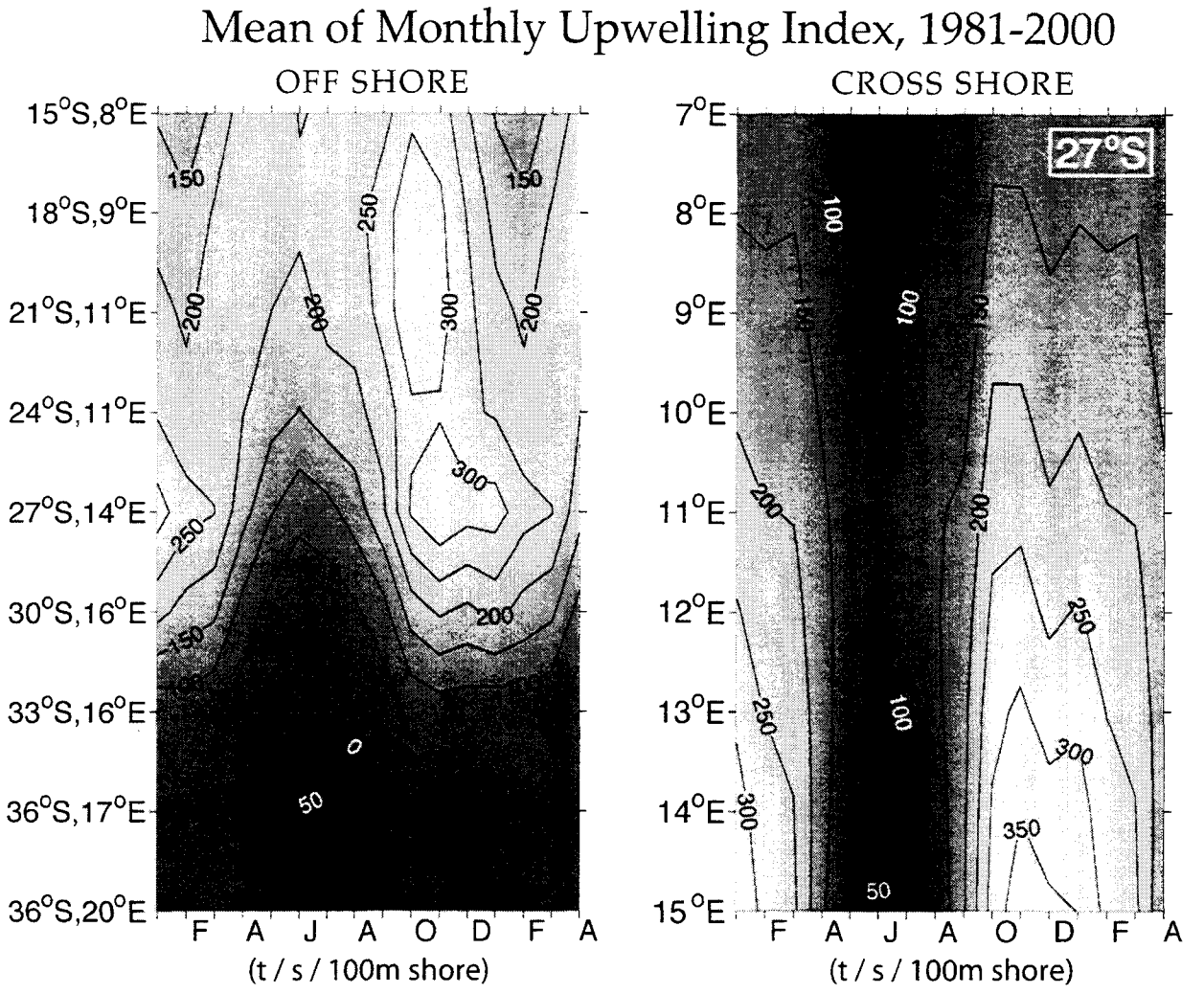

Figure 4. Overall mean (1981-2000) annual cycle of Upwelling Index (UI) summarized for the Offshore and Cross Shore locations 15°-45°S off the southwest coast of Africa. The range of means is from -74 to 382 t/s/100m of coastal length. The abscissa is month, with January at the left. The first four months of the year are repeated on the right. Lighter shading gives larger UI values. Ordinates give latitude for the Offshore points and Longitude for the Cross Shore set. Additional details in Figure 2 and the text.

When mean UI values are examined for a Cross Shore, east-west line of computation points at 27°S, the annual cycle remains in phase, with the highest computed values near shore (Figure 4, right panel). This is in accord with the results of Parrish et al. (1983) who used surface wind observations to compute Ekman transport in this region. We find UI at 27°S more persistent at the most intense level and seasonally less persistent than UI at the more northern computation locations (Figures 4 & 5).

Bakun and Nelson (1991), using a 1° x 1° grid to calculate wind stress curl off southwest Africa, show that the wind curl is positive over a coastal band 200 to 400 km wide from October through May along the entire coast of southwest Africa from 36°S to 24°S. During austral winter (June–August), the band of positive curl may be as wide as 600 km and extends southward only to 33°S. The wind field off Cape Frio region has positive curl throughout the year (Bakun and Nelson, 1991). A northward wind stress field off southwestern Africa need not have positive curl to have positive upwelling index, but increasing UI with distance from shore is consistent with a positive windstress curl field.

Our calculations of UI for the Cross Shore locations at 27°S suggest a wind stress field with

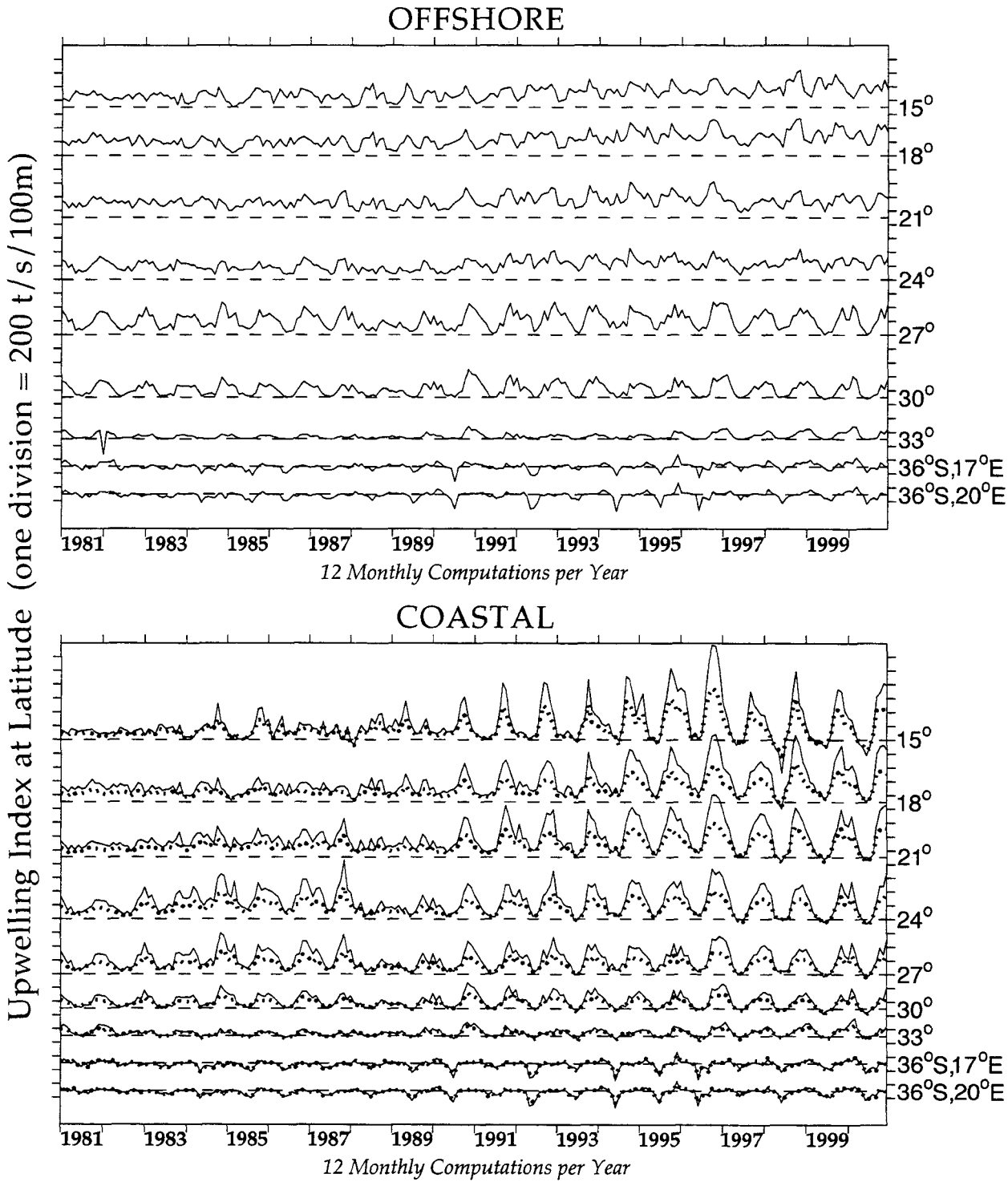

Figure 5. Time series of monthly mean Upwelling Index (UI) computed for 9 locations of the Offshore (upper) and Coastal (lower) series. Solid line gives monthly mean UI computed from monthly mean pressure fields. Dotted line in lower panel shows upwelling index computed from 6-hourly pressure grids, then averaged by month. Dashed line gives a zero reference. Each vertical division represents 200 t/s/100m of coastline. Lower latitudes are toward the top (right).

positive curl during the austral winter (Figure 4, right panel). This UI pattern is compatible with positive curl out to about 11° E, which is near the seaward limit of positive curl shown by Bakun and Nelson (1991). The UI calculations at 27°S for the other seasons (September-March) are not consistent with positive curl, but they are consistent with the offshore Ekman transport (upwelling index) computations of Parrish et al. (1983). The differences may be the result of differences in computation technique and temporal interval used in the climatologies.

Time series of UI for the Offshore computation set (Figure 5, top panel) exhibit distinct annual cycles at 27°S and 30°S. Persistent maxima in the annual cycles (Figure 4, left panel) are clearly evident in the "flattened" tops of the time series for 27°S (Figure 5, upper panel). Offshore time series north of 27°S are "tropical" in that their annual cycles are less distinct (Figure 5). An apparent drift to higher UI after 1990 is seen in the UI series from 24°S to 15°S. The UI series at 33°S has weak but regular annual cycles and few negative values (Figure 5). South of the continent, at 36°S, the annual cycle in UI has low amplitude that is reflected in weak downwelling pulses (50-150 t/s/100m) during winter (Figure 5). These pulses are about 30% the magnitude of those shown by Parrish et al. (1983).

Computations at the Coastal locations will have greater influence from terrestrial seasonality because many computation points (Figure 3) will be over land where more solar energy is converted to infrared radiation. This will heat the lower atmosphere enhancing the thermal low pressure system (Figure 1). This heating increases pressure differences between the continental thermal low and the south Atlantic high atmospheric pressure systems. This will in turn increase computed geostrophic winds (Equations 1-4), wind stress (Equation 5) and computed Ekman transport (Equation 6).

Before 1990, and south of 24°S, the Coastal and Offshore UI values are reasonably comparable (Figure 5, lower panel). North of 27°S, and after 1990, the annual cycles may appear exaggerated in the Coastal computation set (Figure 5, lower panel).

Time series for the Cross Shore set of computation points shows continuity over nearly 900 km (Figure 6, upper panel; Table 2) from 15°E to 7°E. The annual cycle is more pronounced in computations for the nearshore points because of the connection to the continental thermal low. Many anomalies to the annual cycle can be traced through all nine series. For instance the lull in the annual cycle that occurred during the 1988-1989 period is evident in each time series.

Computation of time series for 27°S, 14°E suggests that the UI calculation is not particularly sensitive to changes in coastal angle specification in the UI computation from Equation 6 (Figure 6, lower panel). The lower panel of Figure 6 shows that within a sector of about ±30°, coastal angle specification leads to nearly identical results in this area of persistently positive UI. Many finer scale features remain evident within an angular window of ±70°, but the annual cycle is attenuated at these angular extremes.

The variation of annual cycle over latitude, as defined by a 20-year composite of the monthly means, is regular and well defined (Figures 4 and 7), but the standard deviation of anomalies from these means is less regular (Figure 7). For the Offshore computation set at 10° to 33°S, the highest monthly standard deviation follows the highest overall monthly mean UI in space and time. Another maximum occurs south of 33°S where the average UI is low or negative (Figure 7, top right panel). The lower panels of Figure 7 show the time-space distribution of UI anomaly for each year from 1981 to 2000. The apparent shift to higher UI around 1990 makes negative anomalies more common before 1990 and positive anomalies more common after 1990 in patterns which are more apparent at the more northern locations. However, positive and negative anomalies appear in all 20 panels.

Time-space patterns in UI anomaly may be latitudinal (isopleths or contours tending vertically) or seasonal (contours tending horizontally; Figure 7). The latitudinal pattern, which is the most common pattern in the Benguela Current region, shows uniformity, or persistence, of anomaly throughout the year, e.g., 1985, 1989, 1992. The latitudinal pattern is seen in the top two panels of Figure 7 at 27° to 33°S.

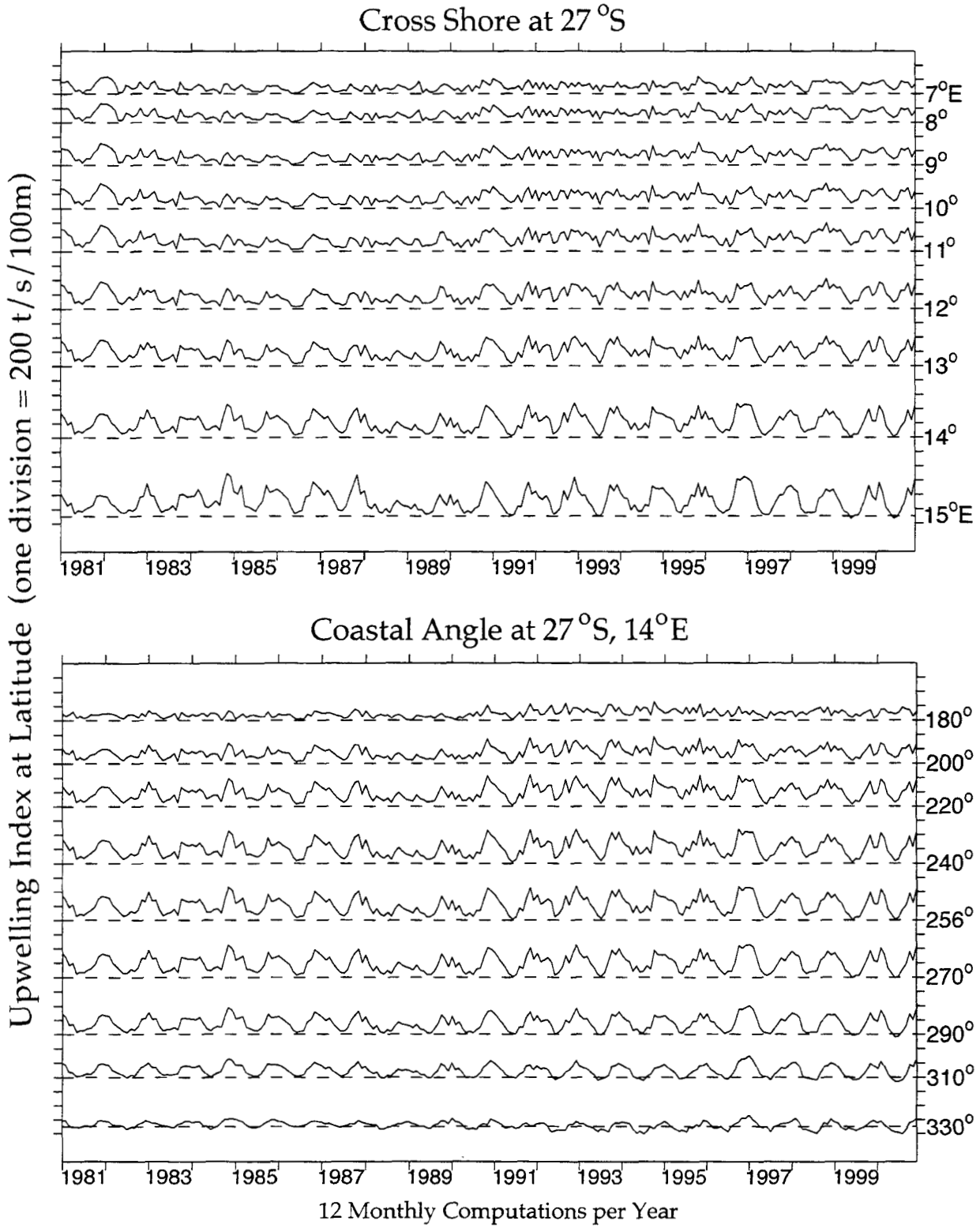

Figure 6. Time series of monthly mean Upwelling Index (UI) computed for 9 locations of the Cross Shore (upper panel) and Coastal Angle (lower panel) series. Solid line gives monthly mean UI computed from monthly mean pressure fields. Dashed line gives a zero reference. Each vertical division represents 200 t/s/100m. Lower latitudes are toward the top (right). Angle of Offshore Ekman transport specified in the UI computation (Equation 6) is given on the right of the lower panel.

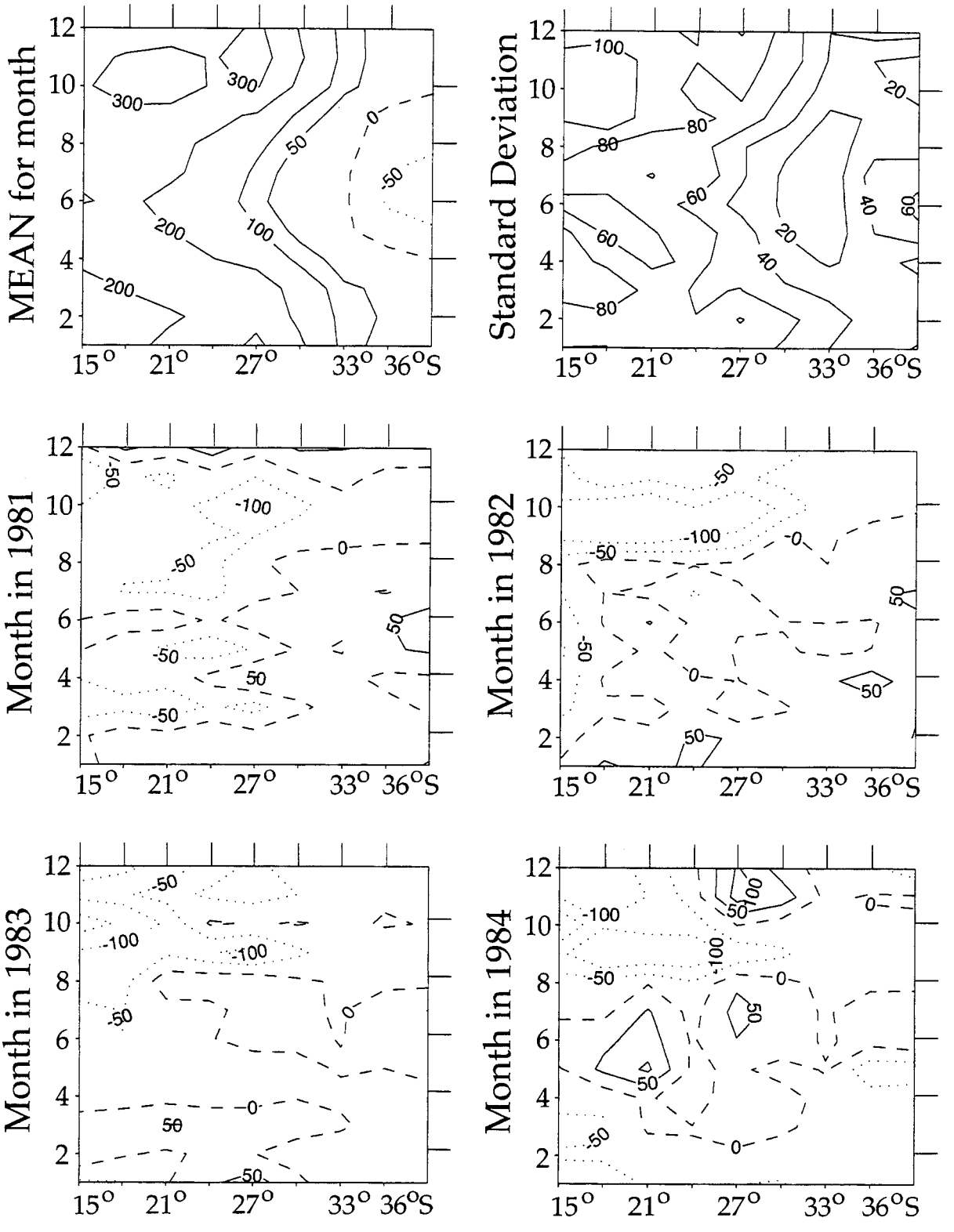

Figure 7. Mean annual cycles are contoured in the upper left panel for the Offshore locations. The overall standard deviation of monthly mean Upwelling Index (UI) is upper right. The lower 20 panels show annual distribution of anomaly for the years 1981 to 2000. Contours are 0, 50, 100, 200 and 300 t/s/100m. Dashed contours show zero UI. Dotted contours show negative anomaly compared to the overall mean. Months are on the ordinate with January at the lower left. Abscissas show latitude from 15° to 45° S.

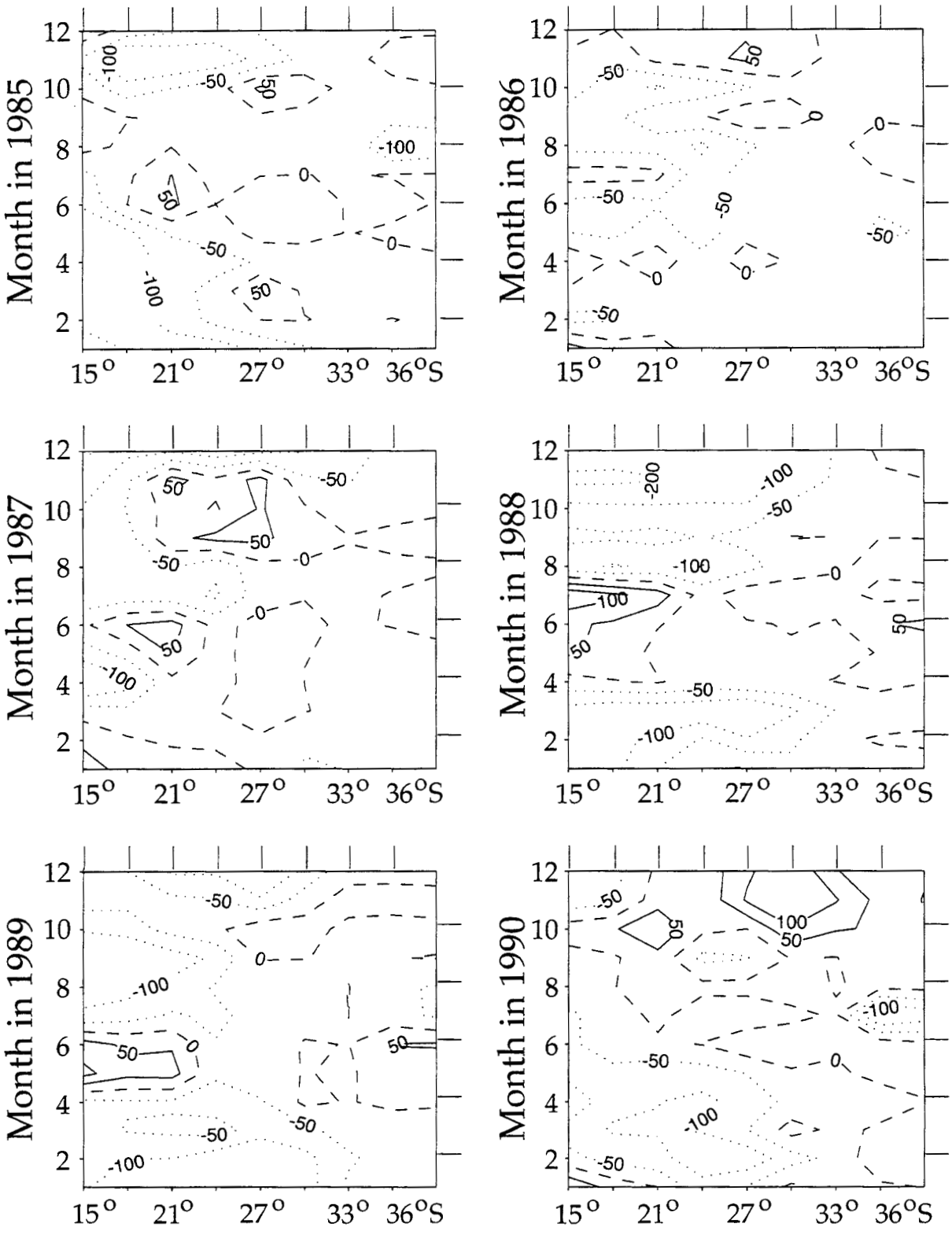

Figure 7 (continued). Mean annual cycles are contoured in the upper left panel for the Offshore locations. The overall standard deviation of monthly mean Upwelling Index (UI) is upper right. The lower 20 panels show annual distribution of anomaly for the years 1981 to 2000. Contours are 0, 50, 100, 200 and 300 t/s/100m. Dashed contours show zero UI. Dotted contours show negative anomaly compared to the overall mean. Months are on the ordinate with January at the lower left. Abscissas show latitude from 15° to 45° S.

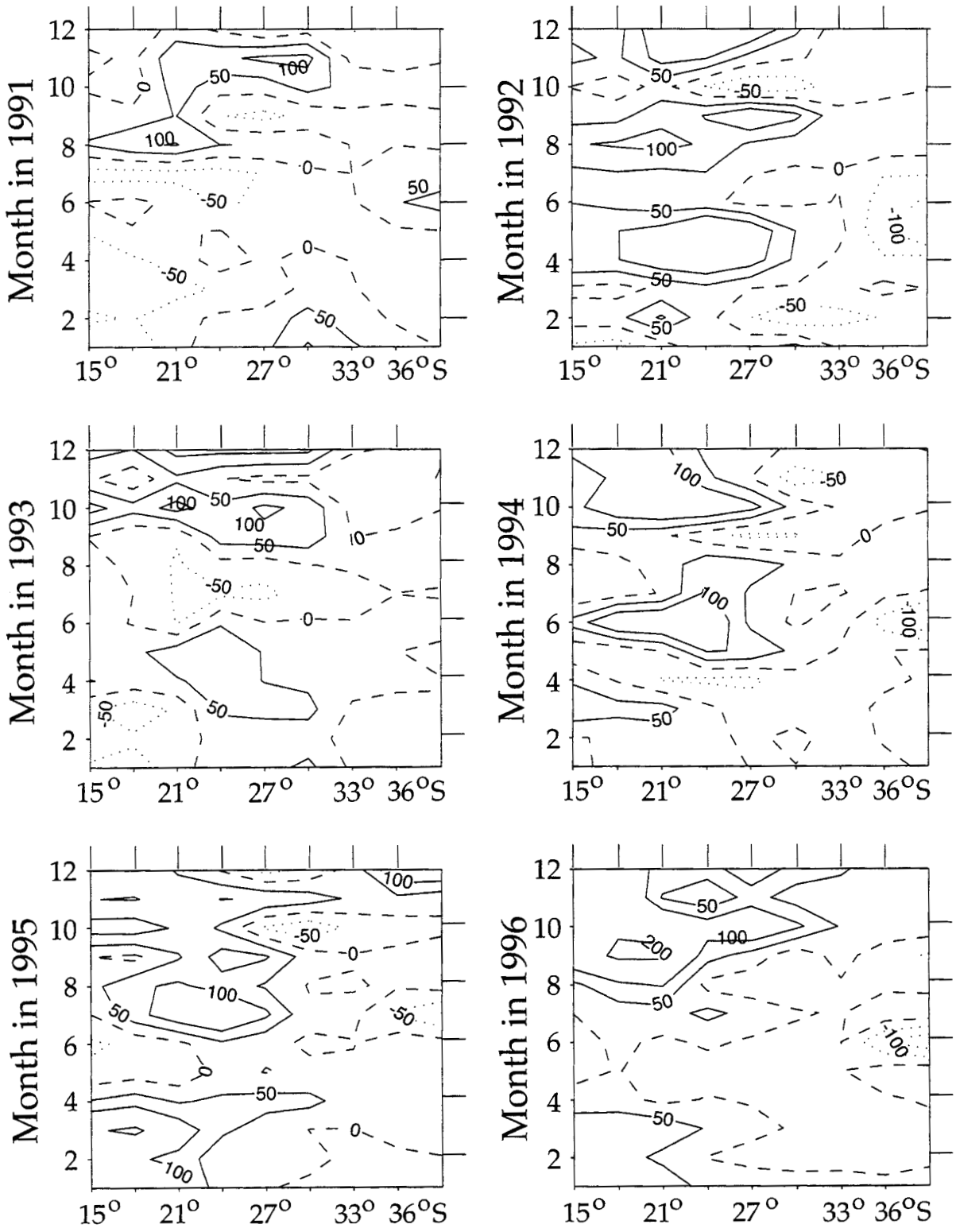

Figure 7 (continued). Mean annual cycles are contoured in the upper left panel for the Offshore locations. The overall standard deviation of monthly mean Upwelling Index (UI) is upper right. The lower 20 panels show annual distribution of anomaly for the years 1981 to 2000. Contours are 0, 50, 100, 200 and 300 t/s/100m. Dashed contours show zero UI. Dotted contours show negative anomaly compared to the overall mean. Months are on the ordinate with January at the lower left. Abscissas show latitude from 15° to 45° S.

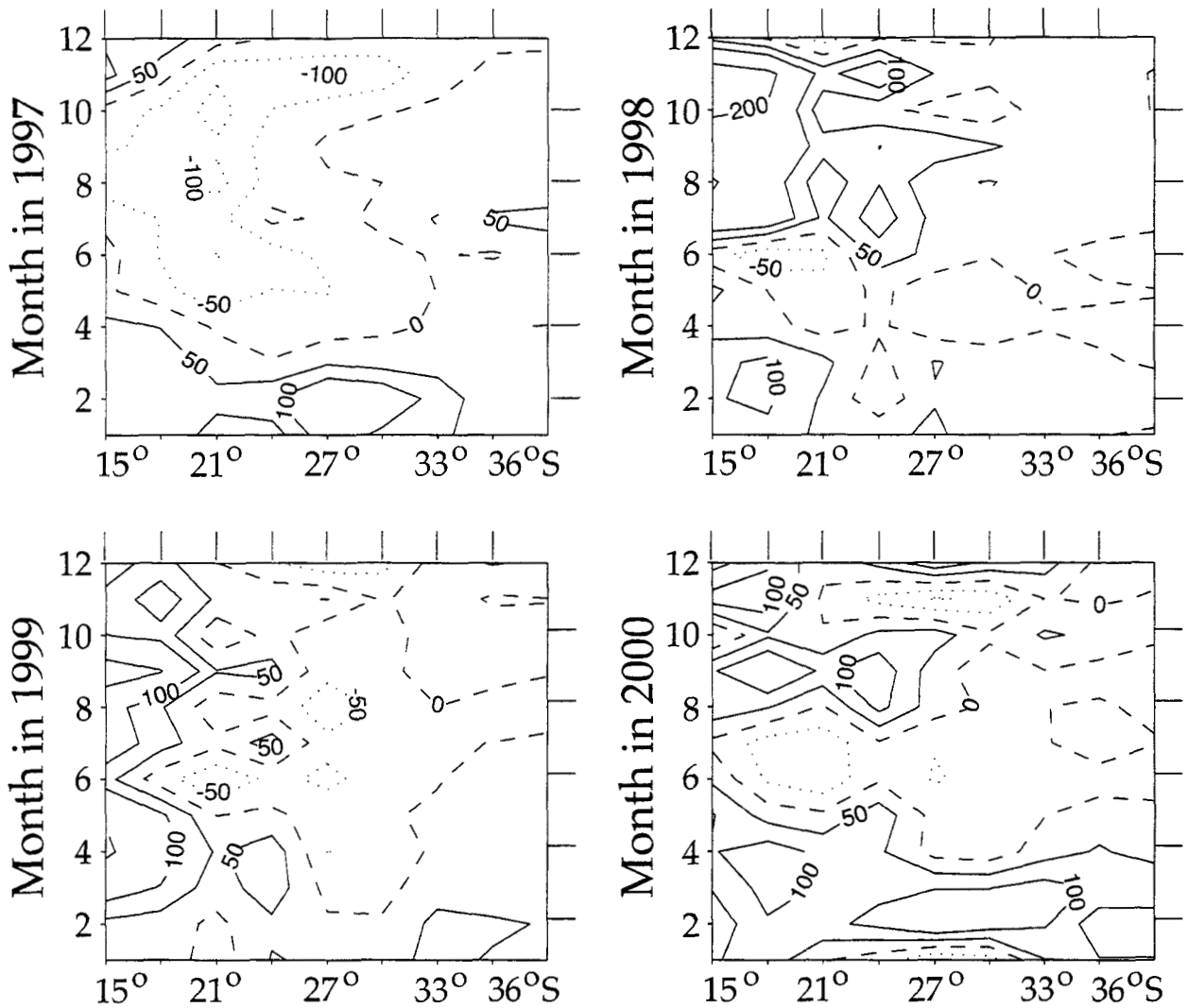

Figure 7 (continued). Mean annual cycles are contoured in the upper left panel for the Offshore locations. The overall standard deviation of monthly mean Upwelling Index (UI) is upper right. The lower 20 panels show annual distribution of anomaly for the years 1981 to 2000. Contours are 0, 50, 100, 200 and 300 t/s/100m. Dashed contours show zero UI. Dotted contours show negative anomaly compared to the overall mean. Months are on the ordinate with January at the lower left. Abscissas show latitude from 15° to 45° S.

Seasonal patterns show uniformity in anomaly over most of the range of latitude (1982, 1988, 1996, 2000) and in the mean, they define the excursion of contours that define the annual UI cycle. During most years both patterns occur together. Near average years also occur when the anomaly contours have low relief and the anomaly has nearly the same sign and magnitude throughout the range of latitude for the entire year, e.g. 1981, 1986, 1991.

Spatial correlation patterns of UI anomaly series are shown in Tables 1 and 2. The closest computation points are generally the most closely related, but latitudinal dependencies are also common. Monthly anomalies at Offshore and Coastal computation points north of 27°S are most closely correlated with their nearest neighbor. Anomalies at the 36°S computation points are similar (r=0.97). Correlation coefficients greater than 0.90 are uncommon at distances greater than 300 km (Tables 1 and 2). Alongshore points over 1000 km distant are seldom highly correlated, but they may be correlated at the $p < 0.05$ level (Table 1). Inverse correlations are not statistically significant.

The Coastal and Offshore time series at 27°S, 30°S and 36°S are highly correlated (r>0.7).

The largest r-values occur where the Offshore and Coastal points are separated by about 100 km. However, the correlation of the 36°S, 17°E Offshore and the 36°S, 20°E Coastal locations is also high. There appears to be partial de-coupling at 30°-33° S (Table 1).

The Cross Shore locations are more highly correlated, within set, than either alongshore station set (Table 2, upper), but the Cross Shore locations are separated by 1° rather than 3° of latitude (Figure 2). Inshore of 27°S, 11°E the UI anomaly time series for the Cross Shore locations are closely related (r>0.9) from 300 to 600 km. Farther offshore at 27°S, r-values greater than 0.9 are found only for 1° latitude separation. The computations for 24S, 11E (Offshore locations) have relatively high correlation to locations 500 km distant in the Cross Shore locations (Table 2, bottom). This suggests that the relationships between adjacent stations in the Cross Shore set may hold at nearby locations to the north.

TABLE 1
CORRELATION OF UI ANOMALIES

Offshore

	15S,08E	*18S,09E*	*21S,11E*	*24S,11E*	*27S,14E*	*30S,16E*	*33S,16E*	*36S,17E*	*36S,20E*
Offshore									
15S,08E	---								
18S,09E	0.88	---							
21S,11E	0.58	0.79	---						
24S,11E	0.48	0.62	0.73	---					
27S,14E		0.36	0.61	0.75	---				
30S,16E			0.38	0.53	0.83	---			
33S,16E		0.33		0.31	0.37	0.50	---		
36S,17E							0.34	---	
36S,20E								0.88	---
Coastal									
15S,12E	0.49	0.57	0.50		0.26				
18S,11E	0.69	0.82	0.67	0.42	0.38		0.38		
21S,13E	0.46	0.61	0.71	0.35	0.53	0.33	0.31		
24S,14E			0.54	0.30	0.70	0.41			
27S,15E			0.50	0.48	0.90	0.67			
30S,17E			0.40	0.42	0.86	0.92	0.39		
33S,17E		0.32		0.35	0.42	0.69	0.71	0.63	0.45
36S,20E								0.88	---
36S,23E								0.78	0.97

Coastal

	15S,12E	*18S,11E*	*21S,13E*	*24S,14E*	*27S,15E*	*30S,17E*	*33S,17E*	*36S,20E*	*36S,23E*
Coastal									
15S,12E	---								
18S,11E	0.85	---							
21S,13E	0.80	0.88	---						
24S,14E	0.45	0.45	0.76	---					
27S,15E	0.28	0.33	0.59	0.89	---				
30S,17E		0.26	0.47	0.66	0.86	---			
33S,17E		0.35				0.47	---		
36S,20E							0.45	---	
36S,23E							0.36	0.97	---

Table 1. Correlation coefficients (r) showing spatial patterns of Upwelling Index (UI) anomaly for the Offshore locations are at the top and coefficients for the intercorrelation of the Coastal stations are at the bottom. Coefficients for the correlation of the Offshore set with the Coastal set are in the middle. Coefficients less than 0.25 are omitted. Coefficients greater than 0.70 are underlined to show event patterns. Nominally, coefficients greater than 0.25 will occur by chance less than five percent of the time (240 monthly samples).

TABLE 2
CORRELATION OF UI ANOMALIES

	Cross Shore									
	27S,06E	27S,07E	27S,08E	27S,09E	27S,10E	27S,11E	27S,12E	27S,13E	27S,14E	27S,15E
Cross Shore										
27S,06E	- - -									
27S,07E	0.99	- - -								
27S,08E	0.96	0.99	- - -							
27S,09E	0.92	0.96	0.99	- - -						
27S,10E	0.86	0.92	0.96	0.99	- - -					
27S,11E	0.80	0.86	0.92	0.96	0.99	- - -				
27S,12E	0.73	0.79	0.85	0.90	0.95	0.98	- - -			
27S,13E	0.60	0.66	0.72	0.77	0.82	0.88	0.95	- - -		
27S,14E	0.40	0.43	0.47	0.51	0.56	0.63	0.74	0.91	- - -	
27S,15E						0.27	0.41	0.66	0.91	- - -

	Cross Shore									
	27S,06E	27S,07E	27S,08E	27S,09E	27S,10E	27S,11E	27S,12E	27S,13E	27S,14E	27S,15E
Offshore										
15S,08E		0.27		0.32	0.34	0.35	0.33	0.28		
18S,09E	0.32	0.37	0.40	0.43	0.45	0.46	0.46	0.43	0.36	
21S,11E		0.28	0.31	0.34	0.38	0.42	0.49	0.58	0.61	0.50
24S,11E	0.52	0.59	0.66	0.72	0.78	0.84	0.87	0.87	0.75	0.48
27S,14E	0.40	0.43	0.47	0.51	0.56	0.63	0.74	0.91	- - -	0.91
30S,16E	0.49	0.52	0.55	0.57	0.59	0.63	0.72	0.82		0.68
33S,16E	0.36	0.39	0.41	0.43	0.43	0.44	0.45	0.43	0.37	
36S,17E	0.46	0.47	0.45	0.43	0.39	0.34	0.27			
36S,20E										

Table 2. Correlation coefficients (r) showing spatial patterns in Upwelling Index (UI) anomaly for the Cross Shore locations are at the top and coefficients for the intercorrelation of the Cross Shore and Offshore locations are at the bottom. Coefficients less than 0.25 are omitted. Coefficients greater than 0.70 are underlined to show patterns of association. Nominally, coefficients greater than 0.25 will occur by chance less than five percent of the time (240 monthly samples).

Biharmonic analysis focuses on annual and semi-annual harmonics of the 1981 to 2000 ensemble of monthly means at each computation point. Computed UI time series for the Offshore computation set are fitted by least-squares to a combination of annual and semi-annual harmonics (Equation 7). The biharmonic fit, a ±1.0 standard error envelope, and the original computed UI points for each offshore computation location are shown in the left panels of Figure 8. Table 3 gives additional analysis detail.

The overall means (Figure 4), time series (Figure 5) and the biharmonic fits (Figure 8, Table 3) show that maximum upwelling occurs in austral spring during months 10-11 (October-November) from 24°S equatorward. South of 24°S the maximum occurs in the austral summer in December-February (Figure 8). This is similar to the spring-to-summer migration of the UI maximum off the west coasts of North and South America (Schwing et al., 1996; Norton et al., 2001) and in agreement with previous studies of the Benguela Current region (Wooster and Reid, 1963). Annual cycle variability decreases and the annual cycle amplitude increases from 15°S to 30°S in the Offshore computation set (Figure 8). At 33°S and poleward the annual cycle decreases in amplitude and negative values appear during the austral winter (May-August). As noted above, the UI is predominately positive north of 30°S and generally becomes increasingly positive as latitude decreases (Figures 4, 5 and 8).

Annual and semi-annual components of the biharmonic fit, adjusted to zero mean, are shown in the right column of Figure 8 for the Offshore computation set. Here it is seen that the spring-to-summer migration of the UI maximum is carried predominately by the annual harmonic. At 15°S the fitted UI maximum is in October (Figure 8, Table 3). At 27°S the annual cycle maximum is in December. The annual harmonic loses amplitude but remains nearly in

phase from 27°S through the higher latitude stations (Figure 8, right). Overall correlation coefficients (r), show the biharmonic fit to be better at 27°-30°S and poleward ($r > 0.62$) than at the more "tropical" northern stations (Table 3). This region of maximum biharmonic fit in the Offshore computation set is near the region where northern and southern extra-seasonal events tend to de-couple (Table 1).

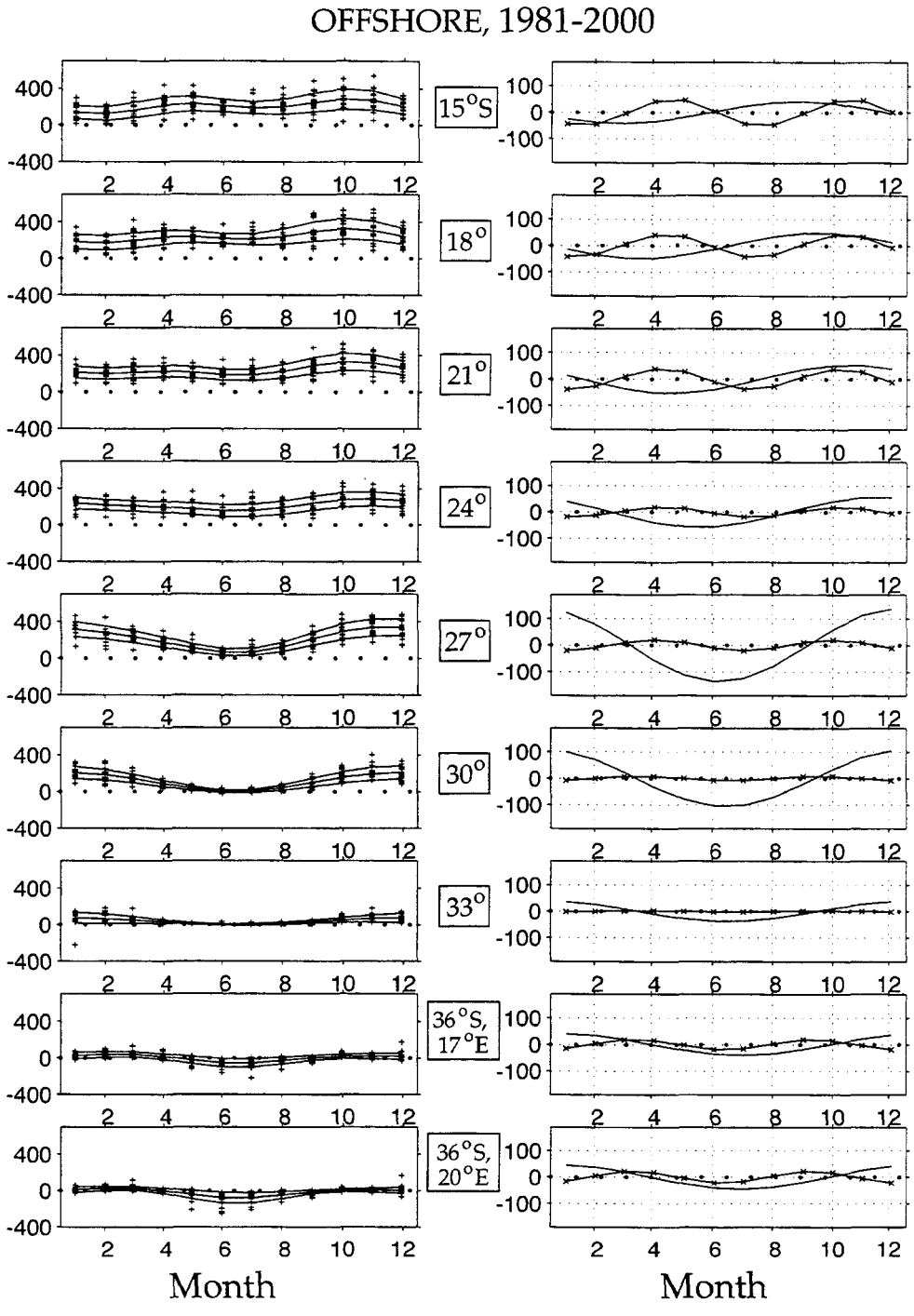

Figure 8. Biharmonic fits to annual and semi-annual cycles within ± 1.0 standard error envelopes of Upwelling Index (UI) computed for the Offshore computation set (left, solid). Symbols (+) show computed UI values of -400 to 600 t/s/100m. Dots give zero reference. Graphs on the right show least squares fitted harmonics with mean adjusted to zero. Values are plotted by month with January on the left. Solid lines show the annual fit and lines with stars (x) show semi-annual fit.

TABLE 3
BIHARMONIC ANALYSIS, SUMMARY FOR 1981 - 2000

Offshore Positions

	15°S, 8°E	18°S, 9°E	21°S, 11°E	24°S, 11°E	27°S, 14°E	30°S, 16°E	33°S, 16°E	36°S, 17°E	36°S, 20°E
Mean, A_0	208.6	238.5	239.4	218.2	212.1	114.1	39.8	1.4	-15.7
r	0.48	0.48	0.55	0.53	0.82	0.84	0.62	0.68	0.70
Maximum UI	286.1	327.7	330.5	287.2	338.3	211.3	75.1	38.9	27.1
Month of Max. UI	10	10	10	11	12	12	12	2	2
Minimum UI	125.3	169.8	186.3	157.2	64.7	1.4	0.8	-54.0	-79.0
Month of Min. UI	2	2	7	6	6	6	6	7	6

Table 3. Biharmonic fit to the Offshore computation set. The rows give the mean value (A_0), overall correlation coefficient (**r**), fitted UI maximum and month of maximum occurrence, fitted UI minimum and month of minimum occurrence. These values correspond to the fitted middle curve in the left column of Figure 7.

DISCUSSION

The major upwelling system components of eastern boundary currents have areas, or centers, where the upwelling process, associated cool water, high nutrient concentration, and elevated primary productivity are persistent (Richards, 1981; Parrish et al., 1983, Nelson, 1977; Strub et al., 1998b; Longhurst, 1998). In the Benguela Current region there are three notable upwelling centers: Cape Frio (18°S), Luderitz (27°S) and the southern Cape region (34°S). In the Offshore computation set, maximum UI is found at 21° to 27°S (Figures 4 and 5). The southern Cape region is strongly influenced by dipole eddies from the Indian Ocean subtropical convergence and the Agulhas retroflection (Strub et al., 1998a; Longhurst, 1998). Upwelling winds are lighter near the Cape than at the northern upwelling centers and the seasonal cycle includes downwelling favorable winds (Figures 4 and 5). At Cape Frio, there is strong upwelling and pronounced seasonal cycles at the Coastal locations and there is continuous positive UI at the Offshore locations (Figures 4 and 5), in agreement with the results of Parrish et al., (1983).

Overall means (Figure 4), anomaly correlation patterns (Tables 1 and 2), and harmonic analysis (Table 3, Figure 8) indicate changes in the seasonal distribution of dominant forcing around the Luderitz upwelling center. Our computations show that upwelling at this location is enhanced by both seasonal (temperate) forcing that extends well offshore (Figure 6, lower panel) and tropical, less seasonal forcing that prolongs the period of maximum upwelling favorable winds (Figures 5 and 6). It is also probable that coastal-trapped waves and currents produced by upwelling of isobars north of 27°S enhance the effects of upwelling at the Luderitz upwelling center and contribute to an elevated level of fixed carbon export at this location (Falkowski, et al., 1998; Longhurst, 1998).

When southwest African UI computations are compared with those for South America (Norton et al., 2001), tropical forcing appears more important off South America where UI is more uniform throughout the year at 15°-21° S. Off South America, UI has a north-south minimum of 50-100 t/s/100m at 18°–24°S (Parrish et al., 1983; Bakun and Nelson, 1991; Norton et al., 2001). This minimum separates temperate annual UI cycles to the south from more tropical UI conditions north of 21°S (Norton et al., 2001). If this minimum exists off southwestern Africa, it is much reduced and the mean UI does not drop below 150 t/s/100m at 21°N (Figure 4, left panel). Off southwest Africa the annual cycle remains strong at the tropical stations (Figures 4, 8), particularly at Coastal locations (Figure 5, lower panel). Migration of the UI maximum poleward in spring is qualitatively similar for the California Current (Mason and Bakun, 1986; Schwing et al., 1996), Peru-Chile Current (Strub et al., 1998a; Norton et al., 2001) and Benguela Current regions (Figure 4).

Upwelling Index Climate Shift: Data Source Comparison

Equatorward of 27°S there is an apparent shift in UI climatology during the 1990-1991 period (Figures 5, 6, 7). FNMOC and National Center for Environmental Prediction (NCEP) data sources were compared to check coherency of the 1990-1991 UI climate shift (Figure 9). Since the main task of FNMOC is operational ocean and weather prediction, new analysis techniques are implemented as improvements are demonstrated. Consequently, the standard PFEL UI presented here is computed from pressure fields analyzed by temporally changing FNMOC analysis programs. NCEP reanalysis wind fields are derived from much of the same data as the FNMOC pressure fields, but NCEP reanalysis fields have the advantage of being produced by consistent sets of analysis algorithms during the 1981-2000 study period.

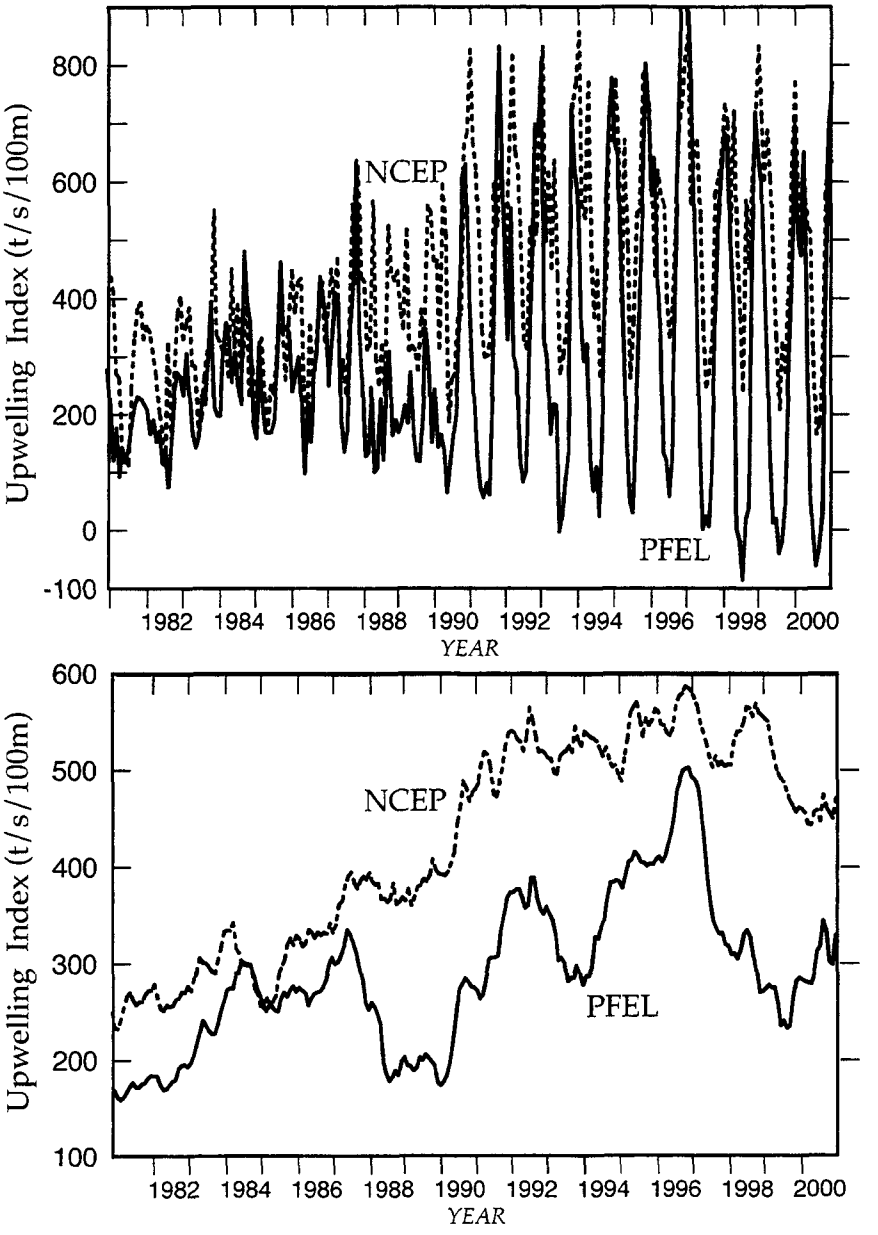

Figure 9. Comparison of PFEL Upwelling Index (UI) to an upwelling index computed from NCEP wind reanalysis data for 21°S, 13°E. The upper panel gives monthly mean values and the lower panel gives these values smoothed by a 12-month running mean. NCEP upwelling index is scaled for comparison. The climate shift in the 1990-1991 period is apparent in both panels.

Comparison of upwelling index time series derived from NCEP winds and PFEL UI for 21°N, 13°E shows general agreement before, during, and after the 1990 to 1991 period (Figure 9). After 1991, annual cycles are more robust in both series. Before 1990, few monthly mean values exceeded 500 t/s/100m. After 1991, higher values occur in every year (Figure 9, upper panel). When the smoothed 12-month running mean of both computations is examined, a transition period is evident in both series (Figure 9, lower panel). The transition in the NCEP series appears to begin in 1980 or before, with the greatest temporal gradient in 1990. The period from 1991 to 1998 had consistently high upwelling index, compared to the pre-1990 interval, in both smoothed series.

The coherent increase in UI during the 1990 to 1991 period and the gross similarity of time series before and after 1990 strongly suggests that the apparent shift in UI is not the result of temporally changing FNMOC analyses. Other differences are seen in the two series (Figure 9), but a complete analysis of these differences is beyond the scope of this Technical Memorandum. Also note that the observed upwelling index climate shift is not the result of differences between upwelling index computations from monthly mean and six-hourly analyzed FNMOC pressure fields (Figure 5, lower panel). However, it may be exaggerated in the UI presented here (see *MEAN ECMWF FIELDS*).

Mean ECMWF fields

There are quantitative differences between mean UI (Figure 4) and mean upwelling index computed from the long-term mean of daily ECMWF wind fields (Hill et al., 1998; Strub et al., 1998b). North of 30°S, UI values for the Coastal computation set may be inflated by a factor of 1.1-2.0. Maxima in Figure 4 may be shifted 3° to 6° equatorward. Bakun (1973, 1975) and Norton et al. (2001) have described this shift in UI extremes for the west coast of North and South America. Shifts in UI maxima may be related to initial assumptions of the Ekman calculation that calls for exact balance between Coriolis and frictional forces, but this effect would be expected to be relatively small south of 18°S (Xie and Hsieh, 1995). An implication of these comparisons is that the UI is most expeditiously used within latitudinal bands and that direct comparison of UI values between latitudes may be misleading (Bakun 1973, 1975), particularly at lower latitudes where the value of the Coriolis parameter, f, is relatively small (Equation 6). However, it is possible to standardize the UI, then compare variability between UI locations (Norton, 1999).

The drag coefficient, $\mathbf{C_d}$, is also important in interpreting the UI. Unless otherwise specified, all UI calculations in this report are from monthly mean pressure fields, and use a doubled drag coefficient, $\mathbf{C_d}$ = 0.0026. Doubling the $\mathbf{C_d}$ value relative to six-hourly computations (Bakun, 1975) is intended to compensate for smoothing of pressure gradients that occurs when the month's six-hourly pressure fields are averaged (Schwing et al., 1996). Reduction of pressure gradients will reduce geostrophic wind speed proportionately (Equations 1 and 2).

Schwing et al. (1996), in Appendix A of their report on UI along the west coast of North America, present monthly climatologies in UI calculated from six-hourly pressure fields and the UI calculated from the monthly mean pressure, as described in this report. Their comparisons show that, because of the non-linear linkage between geostrophic winds and the upwelling index computed from them (Bakun, 1973; Wright and Thompson, 1983), the UI computed from the monthly mean field will be larger in magnitude than the monthly upwelling index computed from six-hourly pressure fields. This effect is seen in the lower panel of Figure 5. Where upwelling favorable winds are persistent, the UI, computed from monthly mean pressure fields, will generally have larger values than monthly mean upwelling index computed from six-hourly pressure fields (Wright and Thompson, 1983; Thompson et al., 1983). This is the reverse of what is found when the same $\mathbf{C_d}$ value is used in each calculation (see *COMPUTATIONS and ANALYSES*).

As the UI of the monthly mean from monthly mean pressure fields increases, differences between the two computation methods increase, with an upper multiplier limit of 2.0, which is the factor that is different in the two UI computations. At UI greater than 50 t/s/100m, $\mathbf{C_d}$ = 0.0026 is too large and accounts for some of the observed distortion in UI space-time fields. Analysis of the data shown in Figure 5 (lower panel) shows that the factors needed to convert UI obtained from monthly mean calculations to upwelling index means obtained from six-hourly calculations, range from 0.6 for

UI-values exceeding 500 to 1.0 for UI-values less than 50 t/s/100m.

FNMOC analyses and PFEL interpolations tend to smooth sea level pressure gradients so that the UI produced represents spatial averaging of 100 to 500 km coastal extent (Table 1). This smoothing (Figure 3) may be valuable in fisheries studies that involve populations occupying areas exceeding 1000 km^2 because scaling similarities may help detect environmental linkages.

Continuity makes the UI especially useful in living marine resource studies. By using global forecasts as analysis initiators, FNMOC uses knowledge of previous conditions and model results to augment problems arising from sampling discontinuities (Rosemond, 1992). This leads to integration on synoptic time scales and provides continuously updated global sea level pressure analyses. Consequently, there are always PFEL UI values available to match the temporal span of sampling programs.

Finally, ocean upwelling, if sufficiently intense and prolonged, enhances nutrient supply to primary producers. If these photosynthetic cells are in the euphotic zone, the critical first step in producing new organic carbon compounds for coastal ecosystems is enabled. Indices of upwelling are closely related to this vital first step and have been used effectively in hundreds of studies which examine differences in ocean productivity at various trophic levels (e.g. Parrish et al., 1981; Norton, 1987; Ainley et al., 1995; VenTresca et al., 1995; Longhurst, 1998).

REFERENCES

Ainley, D. G., W. J. Sydeman and J. G. Norton, Upper trophic level predators indicate interannual negative and positive anomalies in the California current food web, *Mar. Ecol. Prog. Ser., 118*, 69-79, 1995.

Bakun, A., Coastal upwelling indices, west coast of North America, 1946-71, 103 pp., *NOAA Tech. Rep. NMFS SSRF-671*, 1973.

Bakun, A., Daily and weekly upwelling indices, west coast of North America, 1967-73, 114 pp., *NOAA Tech. Rep. NMFS SSRF-693*, 1975.

Bakun, A. and C. S. Nelson, The seasonal cycle of wind-stress curl in subtropical eastern boundary current regions, *J. Phys. Oceanogr., 21*, 1815-1834, 1991.

Clancy, R. M., Operational Modeling: Ocean modeling at the Fleet Numerical Oceanography Center, *Oceanography, 5*, 31-35, 1992.

Cole, J. F .and T., J. McGlade, Temporal and spatial patterning of sea surface temperature in the northern Benguela upwelling system: possible environmental indicators of clupeoid production, *S. Afr. J. Mar. Sci., 19*, 143-158, 1998.

Crawford, R. J. M., Responses of African penguins to regime changes of sardine and anchovy in the Benguela system, *S. Afr. J. Mar. Sci.; 19*: 355-364, 1998.

Cury, P., C. Roy, R. Mendelssohn, A. Bakun, D. M. Husby and R. H. Parrish, Moderate is better: exploring nonlinear clematic effects on the California northern anchovy (Engraulis mordax), 417-424, In R.J. Beamish (Ed.) Climate change and northern fish populations, *Can. Spec. Publ. Fish. Aquat. Sci., 121*, 415-424, 1995.

Davidson, K. L., Observational results on the influence of stability and wind-wave coupling on momentum transfer and turbulent fluctuations over ocean waves, *Boundary-Layer Met. 6*, 305-331, 1974.

Durand, M.-H, P. Cury, R. Mendelssohn, C. Roy, A. Bakun, and D. Pauly, Eds., Global versus local changes in upwelling systems, 593 pp., Orstom Editions, Paris, 1998.

Ekman, V. W., On the influence of the earth's rotation on ocean currents, *Ark. Mat. Astron. Pys. 2*, 1-52, 1905.

Falkowski, P. G., R. T. Barber and V. Smetacek, Biogeochemical controls and feedbacks on ocean primary production, *Science, 281*, 200-206, 1998.

Gill, A. E., Atmosphere - Ocean Dynamics, 662 pp., Academic Press, New York, 1982.

Hill, E. A, B. M. Hickey, F. A. Shillington, P. T. Strub, K. H. Brink, E. D. Barton and A. C. Thomas, Eastern Ocean Boundaries, 29-67 pp., In *The Sea, 11,* A. R. Robinson and K. H. Brink, (Eds.), 1998.

Johnson, A. S. and G. Nelson, Ekman estimates of upwelling at Cape Columbine based on measurements of longshore wind from a 35-year time-series, *S. Afr. J. Mar. Sci., 21*: 433-436, 1999.

Lentz, S. J., The surface boundary layer in coastal upwelling regions, *J. Phys. Oceangr. 22*, 1517-1539. 1992.

Longhurst, A., Ecological geography of the sea, 398 pp., Academic Press, New York, 1998.

Lynn, R. J., Seasonal variation of temperature and salinity at 10 meters in the California current, *Calif. Coop. Ocean. Fish. Invest. Rept., 11*, 157-173, 1967.

Mann, K. H. and J. R. N. Lazier, Dynamics of Marine Ecosystems, Biological-Physical Interactions in the ocean, second edition, 394 pp., Blackwell Science, Cambridge, Massachusetts, 1996.

Mason, J. E. and A. Bakun, Upwelling index update U. S. west coast 33N-48N latitude, 81 pp., *NOAA Tech. Memo. NOAA-TM-NMFS-SWFC-67, 1986.*

Nelson, C. S., Wind stress and wind stress curl over the California Current, *NOAA-TM-NMFS SSRF 714*, pps. 87, 1977.

Norton, J. G., Ocean climate influences on groundfish recruitment in the California current, 73-98 pp., In: Proceedings of the International Rockfish Symposium, October 20-22, 1986, Alaska Sea Grant College Program, Fairbanks, Alaska, 1987.

Norton, J. G., Apparent habitat extensions of dolphinfish (Coryphaena hippurus) in response to climate transients in the California current, *Scientia Marina 63(3-4)*, 239-260, 1999.

Norton, J.G., F.B. Schwing, M. H. Pickett, D. M. Husby and.C.S. Moore, Monthly mean coastal upwelling indices, west coast of South America 1981 to 2000: Trends and relationships, *NOAA Tech. Memo. NOAA-TM-NMFS-SWFC-316*, 2001.

Parrish, R., C. Nelson and A. Bakun, Transport mechanisms and reproductive success of fishes in the California current, *Biol. Oceanog. 1*, 175-203, 1981.

Parrish, R. H, A. Bakun, D. M. Husby and C. S. Nelson, Comparative climatology of selected environmental processes in relation to eastern boundary current pelagic fish reproduction, 731-777 pp., In: Proceedings of the expert consultation to examine changes in abundance and species composition of neritic fish resources, G. D. Sharp and J. Csirke (Eds.), *FAO Fish. Rep., 291*, 3, 1983.

Peterson, W. T. and C. B. Miller, Seasonal cycle of zooplankton abundance and species composition along central Oregon coast, *Fish. Bull. 75,* 717-724, 1977.

Price, J. F. and M. A. Sundermeyer, Stratified Ekman layers, *J. Geophys. Res.,104*, 20,467-20,494, 1999.

Richards, F. A., Ed., Coastal Upwelling, 529 pp., American Geophysical Union, Washington, D. C.,1981.

Rosmond, T. E., A prototype fully coupled ocean-atmosphere prediction system, *Oceanography, 5*, 25-30, 1992.

Ryther, J. H., Photosynthesis and fish production in the sea, *Science, 166*, 72-80, 1969.

Schwing, F. G., M. O'Farrell, J. Steger and K. Baltz, Coastal upwelling indices, west coast of north America 1946-1995, 207 pp., *NOAA Tech. Memo, NOAA-TM-NMFS-SWFSC-231*, 1996.

Schwartzlose, R. A. , J. Alheit, A. Bakun, T. R. Baumgartner, R. Cloete, R. J. M. Crawford, W. J. Fletcher, Y. Green-Ruiz, E. Hagen, T. Kawasaki, D. Lluch-Belda, S.E.. Lluch-Cota, A. D. MacCall, Y. Matsuura, M.O. Nevez-Martinez, R.H. Parrish, C. Roy, R. Serra, K. V. Shurst, M.N Ward and J. Z. Zuzunaga, Worldwide large-scale fluctuations of sardine and anchovy populations, *S. Afr. J. Mar. Sci., 21*, 289-248, 1999.

Smith, R. L., Upwelling, *Oceanogr. Mar. Biol. Ann. Rev., 6*, 11-46, 1968.

Strub, P. T., F. A. Shillington, C. James and S. J. Weeks, Satellite comparison of seasonal circulation in the Benguela and California current systems, *S. Afr. J. Mar. Sci., 19*, 99-112, 1998a.

Strub, P. T, J. M. Mesias, V. Montecino and J. Rutllant, Coastal ocean circulation of western South America, 273-313 pp. In: *The Sea, Volume 11*, A. R. Robinson and K. H. Brink (Eds.), 1998b.

Sverdrup, H. U., M. W. Johnson and R. H. Fleming, The Oceans, their physics, chemistry and general biology, 1087 pp., Prentice-Hall, New Jersey, 1942.

Thomas, A. C., F. Huang, P. T. Strub and C. James, Comparison of the seasonal and interannual variability of phystoplankton pigment concentrations in the Peru and California Current systems., *J. Geophys. Res. 99*, 7355-7370, 1994.

Thompson, K. R., R. F. Marsden and D. G. Wright, Estimation of low-frequency wind stress fluctuations of the open ocean, *J. Phys. Oceanog., 13*, 1003-1011, 1983.

Traganza, E., J. C. Conrad and L. C. Breaker, Satellite observations of a cyclonic upwelling system and giant plume in the California Current, *In* Coastal Upwelling, American Geophysical Union, F. A. Richards (Ed.), 228-241, 1981.

VenTresca, D. A., R. H. Parrish, J. L. Houk, M. L. Gingras, S. D. Short and N. L. Crane, El Niño effects on the somatic reproductive condition of blue rockfish, Sebastes mystinus, *Calif. Coop. Oceanic Fish Invest. Rep. 36*, 167-174, 1995.

Waldron, H. N. and T. A. Probyn, Nitrate supply and potential new production in the Benguela upwelling system, *S. Afr. J. Mar. Sci., 12*, 29-39, 1992.

Wooster, W. S. and J. L. Reid, Jr., Eastern Boundary Currents, 253-280 pp., M. N. Hill, Ed., *The Sea, Vol. 2*, Interscience, New York, 1963.

Wright, D. G. and K. R. Thompson, Time-averaged forms of the nonlinear stress law, *J. Phys. Oceanog., 13*, 341-345, 1983.

Xie, L and W. W. Hseih, The global distribution of wind-induced upwelling, *Fish. Oceanogr., 4*, 52-67, 1995.

APPENDIX I

TABLES OF MONTHLY MEAN UPWELLING INDEX VALUES
FOR COASTAL AND OFFSHORE COMPUTATION SETS

Offshore Upwelling Index (t/s/100m coast)

Year	Month	15°S, 8°E	18°S, 9°E	21°S, 11°E	24°S, 11°E	27°S, 14°E	30°S, 16°E	33°S, 16°E	36°S, 17°E	36°S, 20°E
1981	1	125	209	240	292	352	233	111	46	4
1981	2	110	187	208	260	289	208	122	89	53
1981	3	88	141	136	170	184	150	78	55	18
1981	4	176	214	204	218	224	113	37	6	-7
1981	5	240	190	139	88	59	32	5	20	18
1981	6	197	235	216	139	92	31	11	-9	-18
1981	7	192	180	156	110	67	13	12	-54	-53
1981	8	173	193	173	125	111	62	26	20	5
1981	9	192	260	245	174	137	48	8	-35	-44
1981	10	241	335	306	233	191	110	37	10	2
1981	11	172	265	264	274	299	203	98	-1	-10
1981	12	194	305	293	336	339	244	123	65	35
1982	1	149	241	249	305	327	230	-222	66	30
1982	2	104	176	204	273	315	216	107	67	25
1982	3	98	201	208	229	218	156	71	57	29
1982	4	136	248	250	205	169	92	64	94	23
1982	5	126	200	208	151	107	31	2	-23	-21
1982	6	112	217	237	137	61	7	6	-64	-49
1982	7	158	235	200	122	74	34	14	-8	-18
1982	8	183	264	239	189	133	60	12	-17	-33
1982	9	118	138	131	116	103	82	15	4	6
1982	10	182	201	194	190	144	87	36	11	1
1982	11	205	299	276	275	289	172	65	8	-10
1982	12	159	235	249	243	257	122	36	-32	-35
1983	1	87	130	210	283	397	231	40	-20	-12
1983	2	161	167	184	224	272	157	47	5	-9
1983	3	203	241	275	261	284	182	66	19	-2
1983	4	176	214	213	169	149	78	14	6	-1
1983	5	217	206	173	124	64	15	12	-24	-37
1983	6	164	161	159	143	95	20	4	-39	-52
1983	7	174	182	192	161	107	24	1	-14	-27
1983	8	121	165	247	224	159	48	6	-37	-50
1983	9	145	215	211	125	71	18	4	-28	-39
1983	10	37	155	259	296	301	175	54	29	6
1983	11	210	255	287	235	277	157	56	16	2
1983	12	66	128	182	234	259	158	62	4	-1
1984	1	49	111	168	234	273	163	47	7	4
1984	2	76	116	169	211	251	147	47	16	11
1984	3	85	148	231	215	300	174	33	27	7
1984	4	211	206	240	163	215	101	9	-7	-12
1984	5	231	284	309	161	112	12	10	-108	-124
1984	6	242	248	258	142	112	35	0	-40	-53
1984	7	193	218	266	161	150	47	0	-19	-36
1984	8	173	202	213	146	163	56	1	-33	-50
1984	9	147	114	120	75	102	22	0	-60	-54
1984	10	292	246	269	213	305	143	26	10	-2
1984	11	171	160	223	268	469	286	64	25	10
1984	12	84	108	186	245	425	215	50	-18	-68
1985	1	69	80	95	114	236	161	37	7	1
1985	2	4	38	107	182	270	182	65	43	17
1985	3	19	59	159	176	314	150	31	10	-5
1985	4	61	103	158	138	123	37	5	-8	-11
1985	5	58	108	153	135	127	54	4	-9	-15
1985	6	108	210	244	148	99	23	4	-84	-86
1985	7	144	224	262	150	81	14	4	-48	-74
1985	8	221	223	215	146	114	19	5	-128	-125
1985	9	278	282	263	193	180	60	12	-43	-50
1985	10	269	262	298	266	365	204	41	9	2
1985	11	217	136	166	163	259	169	54	42	37
1985	12	236	223	221	181	277	148	41	13	1

Year	Month	15°S, 8°E	18°S, 9°E	21°S, 11°E	24°S, 11°E	27°S, 14°E	30°S, 16°E	33°S, 16°E	36°S, 17°E	36°S, 20°E
1986	1	216	203	235	211	310	187	50	11	0
1986	2	51	105	166	179	265	157	35	16	2
1986	3	160	171	212	174	228	117	22	9	-1
1986	4	268	236	257	169	191	76	9	2	-4
1986	5	187	161	177	92	90	23	-1	-88	-84
1986	6	134	132	128	81	33	0	-1	-95	-99
1986	7	232	260	225	96	54	6	-1	-52	-71
1986	8	134	159	140	79	61	16	2	-2	-10
1986	9	154	218	258	214	229	96	11	-19	-41
1986	10	271	257	241	211	251	161	50	8	-6
1986	11	258	273	338	326	409	230	65	16	-5
1986	12	239	243	289	294	362	196	65	1.5	-16
1987	1	219	213	240	262	314	161	30	-13	-27
1987	2	155	166	184	205	258	137	37	-8	-9
1987	3	145	170	218	211	295	162	45	11	-1
1987	4	52	119	216	168	208	80	8	-5	-10
1987	5	160	191	251	147	134	28	6	-50	-61
1987	6	187	261	254	130	82	15	0	-54	-66
1987	7	124	159	133	70	58	12	-1	-49	-65
1987	8	120	149	169	98	106	34	2	-33	-44
1987	9	143	211	308	283	253	98	23	1	-9
1987	10	198	290	369	285	361	179	32	8	0
1987	11	138	247	392	307	414	165	22	-1	-4
1987	12	111	133	160	128	209	85	16	-25	-22
1988	1	13	69	164	234	330	179	36	-8	-15
1988	2	16	49	101	170	174	119	65	48	38
1988	3	46	68	90	75	90	51	10	1	1
1988	4	204	238	236	180	166	77	25	38	3
1988	5	293	258	184	149	82	22	0	-23	-19
1988	6	255	253	187	126	59	12	3	-11	-30
1988	7	350	346	288	158	112	37	25	-66	-90
1988	8	119	129	123	85	52	19	5	-10	-18
1988	9	193	236	236	167	155	81	20	-14	-27
1988	10	221	257	262	206	220	132	30	6	-17
1988	11	52	86	116	127	175	131	30	12	4
1988	12	67	91	120	105	141	83	26	31	23
1989	1	47	69	92	87	127	90	40	10	5
1989	2	37	61	91	85	99	64	18	14	12
1989	3	93	160	184	182	183	97	31	11	-1
1989	4	160	185	174	127	113	91	21	31	9
1989	5	351	289	269	128	93	29	3	-7	-9
1989	6	270	251	228	101	46	11	5	-5	-36
1989	7	120	162	167	117	51	1	7	-83	-135
1989	8	77	112	132	144	87	10	13	-68	-89
1989	9	58	104	144	130	192	81	11	-15	-24
1989	10	197	263	314	280	340	195	43	7	-5
1989	11	248	272	283	249	256	181	99	40	24
1989	12	206	195	157	152	151	105	51	6	-12
1990	1	240	212	214	161	276	226	63	12	10
1990	2	81	92	107	85	134	110	41	81	74
1990	3	92	101	119	117	202	180	46	47	56
1990	4	220	155	133	87	93	43	6	-2	-1
1990	5	166	161	116	97	56	22	1	-12	-20
1990	6	138	185	174	150	100	39	12	-27	-81
1990	7	152	205	225	146	49	1	13	-219	-208
1990	8	173	230	255	203	138	64	8	-9	-19
1990	9	213	273	304	156	136	84	19	12	4
1990	10	318	381	438	304	306	263	114	71	12
1990	11	192	245	351	304	454	403	180	51	2
1990	12	129	180	274	274	410	334	125	23	14

Year	Month	15°S, 8°E	18°S, 9°E	21°S, 11°E	24°S, 11°E	27°S, 14°E	30°S, 16°E	33°S, 16°E	36°S, 17°E	36°S, 20°E
1991	1	54	93	195	280	359	322	136	44	7
1991	2	74	107	175	226	289	249	99	34	14
1991	3	94	121	155	171	219	176	61	24	20
1991	4	136	182	201	228	161	98	22	-6	-4
1991	5	190	219	195	173	64	11	0	-31	-41
1991	6	200	225	170	94	19	1	0	-12	-18
1991	7	139	162	144	106	36	3	7	-38	-64
1991	8	257	324	319	239	168	78	9	-22	-40
1991	9	269	300	322	173	124	45	8	-28	-34
1991	10	281	302	424	308	326	240	93	47	36
1991	11	290	298	410	383	458	322	61	2	-2
1991	12	174	200	285	249	272	168	17	-18	-3
1992	1	86	107	190	280	355	278	68	16	3
1992	2	141	194	300	232	221	87	11	-6	-1
1992	3	154	188	234	248	252	154	45	54	24
1992	4	322	338	375	364	299	122	12	-24	-31
1992	5	323	322	318	367	254	78	24	-120	-210
1992	6	245	244	200	160	47	-1	8	-129	-197
1992	7	247	281	249	226	85	6	4	-98	-122
1992	8	300	339	333	280	164	63	31	13	-6
1992	9	262	311	355	321	351	195	31	-2	-17
1992	10	289	309	364	237	214	95	38	18	6
1992	11	338	350	442	398	376	210	66	15	3
1992	12	243	272	416	424	480	252	39	-30	-24
1993	1	86	107	190	280	355	278	68	16	3
1993	2	99	120	171	232	284	203	55	13	5
1993	3	121	122	183	271	320	225	51	23	21
1993	4	276	274	277	270	218	119	42	31	4
1993	5	246	261	279	238	152	41	8	-22	-59
1993	6	212	208	132	196	66	13	7	-14	-52
1993	7	252	233	154	121	20	-14	-3	-52	-85
1993	8	228	218	160	167	93	39	15	0	-9
1993	9	230	233	224	294	271	164	19	-6	-3
1993	10	411	407	466	355	418	257	46	3	5
1993	11	284	273	361	297	333	195	50	6	6
1993	12	274	293	381	373	436	301	76	17	5
1994	1	140	188	255	275	320	215	50	10	16
1994	2	114	165	217	228	260	193	55	46	62
1994	3	255	277	295	224	229	133	41	48	42
1994	4	266	235	178	142	107	63	9	11	6
1994	5	202	190	202	274	199	63	2	-25	-35
1994	6	265	374	352	318	99	-1	32	-129	-252
1994	7	167	212	214	289	123	12	4	-36	-83
1994	8	158	221	232	276	197	81	18	11	0
1994	9	267	305	280	186	128	25	5	-3	-7
1994	10	376	478	518	457	428	202	54	12	4
1994	11	342	422	461	357	348	130	23	-22	-26
1994	12	319	361	379	292	333	181	54	9	11
1995	1	299	342	352	252	326	207	67	4	7
1995	2	226	269	275	227	286	191	66	25	24
1995	3	355	422	360	273	276	159	57	69	66
1995	4	279	319	277	261	239	146	45	36	13
1995	5	199	201	161	188	102	35	14	23	-1
1995	6	138	173	170	188	73	3	4	-26	-71
1995	7	209	313	351	357	194	23	19	-109	-182
1995	8	240	323	326	265	165	36	8	-15	-13
1995	9	234	267	314	343	296	103	24	0	-4
1995	10	414	465	439	331	249	84	24	3	-3
1995	11	327	358	383	396	442	284	115	57	21
1995	12	254	312	311	255	251	148	91	174	165

Year	Month	15°S, 8°E	18°S, 9°E	21°S, 11°E	24°S, 11°E	27°S, 14°E	30°S, 16°E	33°S, 16°E	36°S, 17°E	36°S, 20°E
1996	1	199	255	297	274	362	242	96	30	20
1996	2	202	233	228	213	247	154	60	26	21
1996	3	261	299	309	258	271	152	38	31	15
1996	4	235	258	218	205	164	71	10	14	6
1996	5	227	225	176	150	99	23	6	-2	-9
1996	6	180	219	175	156	57	-4	6	-160	-235
1996	7	210	257	239	242	114	18	2	-10	-40
1996	8	243	322	321	170	92	4	6	-38	-56
1996	9	386	496	484	290	217	47	41	-46	-80
1996	10	418	524	526	419	477	283	105	69	39
1996	11	413	499	367	304	416	233	94	26	6
1996	12	330	398	341	331	465	267	131	38	11
1997	1	213	270	243	266	461	303	147	23	11
1997	2	181	253	257	309	447	332	153	61	28
1997	3	260	290	253	216	296	188	89	74	54
1997	4	289	289	224	181	145	69	31	22	0
1997	5	245	189	110	121	51	11	8	9	-3
1997	6	216	156	82	74	26	0	9	-62	-75
1997	7	195	182	145	190	73	20	6	6	-9
1997	8	129	141	100	159	114	40	19	-8	-29
1997	9	187	223	179	192	199	103	33	20	9
1997	10	267	277	225	242	288	168	67	33	17
1997	11	395	332	230	209	239	122	60	30	14
1997	12	293	324	283	259	323	175	60	13	3
1998	1	224	272	249	281	382	235	95	24	-1
1998	2	214	268	235	177	316	196	121	91	69
1998	3	251	320	289	198	306	191	85	49	16
1998	4	252	261	208	209	136	46	20	4	-2
1998	5	298	222	162	182	69	3	13	-14	-38
1998	6	166	124	123	222	101	11	10	-84	-127
1998	7	385	390	252	309	115	21	18	-8	-53
1998	8	411	371	229	285	129	38	25	4	-20
1998	9	374	469	340	320	277	136	49	12	-9
1998	10	506	529	364	304	289	139	85	63	4
1998	11	540	532	400	449	394	225	122	43	1
1998	12	236	236	189	254	312	183	118	71	34
1999	1	191	214	186	298	361	239	150	64	36
1999	2	152	185	180	254	278	185	142	103	72
1999	3	301	303	246	294	237	145	85	41	32
1999	4	438	378	275	282	119	33	40	51	16
1999	5	429	334	199	181	79	17	22	19	-7
1999	6	266	181	91	111	4	-24	0	-17	-48
1999	7	351	306	224	251	45	-4	5	-51	-57
1999	8	333	288	178	170	42	0	11	-45	-88
1999	9	484	485	323	287	153	57	57	9	-17
1999	10	393	417	307	307	263	139	97	56	18
1999	11	338	443	361	334	399	201	103	12	3
1999	12	233	313	264	213	234	118	98	75	48
2000	1	189	258	220	214	229	140	127	74	61
2000	2	134	254	279	329	439	311	183	56	44
2000	3	218	326	318	301	349	259	179	132	118
2000	4	320	370	318	260	149	50	51	74	31
2000	5	340	252	210	251	84	5	6	2	-5
2000	6	237	152	93	141	9	-23	-2	-82	-139
2000	7	197	161	126	172	36	-7	2	-18	-74
2000	8	290	286	211	303	144	31	11	-16	-47
2000	9	326	456	359	356	210	48	19	-31	-74
2000	10	234	379	352	356	381	182	116	65	26
2000	11	400	447	310	228	242	119	77	12	9
2000	12	234	335	282	322	459	273	145	7	-7

Overall Mean Monthly Offshore Values

Month	15°S, 8°E	18°S, 9°E	21°S, 11°E	24°S, 11°E	27°S, 14°E	30°S, 16°E	33°S, 16°E	36°S, 17°E	36°S, 20°E
1	144.8	182.1	214.2	244.1	322.6	216.0	61.8	21.2	8.2
2	116.6	160.3	191.9	215.0	269.7	179.9	76.4	41.0	27.6
3	164.9	206.4	223.7	213.2	252.7	160.0	58.2	39.6	25.5
4	223.9	241.1	231.6	201.3	169.4	80.3	24.0	18.4	1.4
5	236.4	223.2	199.6	169.9	103.9	27.8	7.3	-24.3	-39.0
6	196.6	210.5	183.7	147.9	64.0	8.4	5.9	-57.2	-89.2
7	209.6	233.4	210.6	177.7	82.2	13.4	6.9	-51.3	-77.3
8	204.2	233.0	215.8	187.7	121.6	39.9	11.7	-21.7	-37.1
9	233.0	279.8	270.0	219.8	189.2	79.7	20.5	-13.6	-25.7
10	290.8	336.7	346.8	290.0	305.9	171.9	59.4	26.9	7.3
11	276.5	309.6	321.1	294.2	347.4	206.9	75.2	19.5	4.3
12	204.0	244.3	263.1	258.2	319.7	187.8	71.2	21.2	8.1

Coastal Upwelling Index (t/s/100m coast)

Year	Month	15°S, 12°E	18°S, 11°E	21°S, 13°E	24°S, 14°E	27°S, 15°E	30°S, 17°E	33°S, 17°E	36°S, 20°E	36°S, 23°E
1981	3	78	138	104	119	150	110	118	18	4
1981	4	155	214	166	173	194	90	43	-7	-10
1981	5	142	177	106	55	43	20	23	18	9
1981	6	111	221	170	101	77	22	6	-18	-22
1981	7	128	185	125	93	63	11	-7	-53	-41
1981	8	133	196	152	116	99	48	34	5	0
1981	9	141	264	201	152	126	41	3	-44	-49
1981	10	148	325	232	184	160	85	53	2	0
1981	11	107	264	211	270	283	180	91	-10	-4
1981	12	82	270	200	272	294	195	159	35	22
1982	1	89	225	186	262	284	183	152	30	17
1982	2	95	180	171	251	273	170	144	25	11
1982	3	77	189	156	182	182	113	120	29	12
1982	4	105	247	201	177	147	65	76	23	6
1982	5	74	204	169	139	97	25	1	-21	-20
1982	6	169	255	203	104	52	6	-7	-49	-35
1982	7	141	228	155	56	52	19	11	-18	-24
1982	8	124	238	158	100	99	43	10	-33	-41
1982	9	76	118	84	60	77	59	47	6	1
1982	10	124	188	142	138	114	60	47	1	0
1982	11	136	274	229	271	270	153	69	-10	-10
1982	12	161	254	249	337	277	131	27	-35	-26
1983	1	56	123	227	461	459	262	47	-12	-6
1983	2	147	168	203	302	291	164	50	-9	-5
1983	3	124	236	281	341	285	165	79	-2	-2
1983	4	73	183	216	216	151	70	25	-1	-2
1983	5	208	208	171	100	54	9	0	-37	-37
1983	6	210	159	143	125	88	18	-1	-52	-51
1983	7	157	178	166	140	96	20	0	-27	-32
1983	8	170	183	231	214	149	42	3	-50	-58
1983	9	184	227	202	168	87	23	0	-39	-37
1983	10	73	147	255	350	305	160	79	6	1
1983	11	210	282	361	409	309	161	64	2	1
1983	12	13	85	172	305	272	157	57	-1	-2
1984	1	42	95	162	294	283	162	60	4	2
1984	2	28	88	167	313	285	155	58	11	14
1984	3	34	121	275	470	376	189	64	7	3
1984	4	120	229	343	401	284	121	12	-12	-10
1984	5	143	287	353	272	134	17	-15	-124	-115
1984	6	198	276	277	190	124	38	0	-53	-55
1984	7	224	265	326	261	171	51	1	-36	-49
1984	8	161	207	257	296	218	76	0	-50	-59
1984	9	205	156	202	260	152	40	-5	-54	-37
1984	10	517	344	442	585	416	179	27	-2	-1
1984	11	255	196	346	657	596	328	102	10	3
1984	12	224	158	291	625	559	261	38	-68	-78
1985	1	103	79	151	374	349	213	49	1	1
1985	2	-2	23	122	313	313	191	90	17	10
1985	3	64	80	279	548	437	188	23	-5	-8
1985	4	6	107	193	232	144	42	1	-11	-7
1985	5	6	88	159	179	131	51	6	-15	-20
1985	6	-2	121	192	157	103	24	-3	-86	-76
1985	7	36	180	209	127	73	11	-1	-74	-74
1985	8	68	174	197	218	143	29	-12	-125	-113
1985	9	214	287	282	301	218	74	3	-50	-39
1985	10	441	354	418	526	432	218	59	2	1
1985	11	460	237	297	413	330	182	74	37	41
1985	12	232	276	322	442	355	171	41	1	0

Year	Month	15°S, 12°E	18°S, 11°E	21°S, 13°E	24°S, 14°E	27°S, 15°E	30°S, 17°E	33°S, 17°E	36°S, 20°E	36°S, 23°E
1986	1	288	270	314	417	380	216	60	0	0
1986	2	9	88	205	396	338	185	54	2	1
1986	3	113	179	256	356	289	139	31	-1	-2
1986	4	217	270	306	315	240	92	7	-4	-4
1986	5	341	231	228	184	119	36	-7	-84	-78
1986	6	44	110	104	79	34	1	-28	-99	-88
1986	7	132	263	240	149	66	10	-7	-71	-75
1986	8	106	143	157	140	79	22	1	-10	-13
1986	9	55	178	254	337	271	112	8	-41	-41
1986	10	244	262	285	353	292	169	62	-6	-2
1986	11	208	278	394	577	482	247	87	-5	0
1986	12	208	278	394	577	482	247	87	-5	0
1987	1	214	237	309	447	378	192	36	-27	-22
1987	2	157	174	213	314	289	147	33	-9	-5
1987	3	157	199	294	435	363	182	54	-1	-2
1987	4	63	162	350	447	282	100	8	-10	-13
1987	5	260	277	367	330	177	37	-5	-61	-63
1987	6	40	201	221	143	81	13	-4	-66	-71
1987	7	103	142	146	115	72	15	-5	-65	-68
1987	8	138	153	187	187	134	43	0	-44	-44
1987	9	222	211	318	402	284	98	22	-9	-16
1987	10	9	224	401	551	440	196	48	0	0
1987	11	5	226	560	859	579	221	24	-4	-4
1987	12	184	181	298	425	306	124	8	-22	-11
1988	1	-28	53	202	382	354	184	44	-15	-20
1988	2	-74	23	88	156	144	87	91	38	23
1988	3	78	93	122	135	101	52	16	1	1
1988	4	205	259	249	240	172	71	33	3	-4
1988	5	133	217	113	59	57	13	0	-19	-20
1988	6	109	204	128	61	42	6	0	-30	-44
1988	7	304	350	269	139	102	32	4	-90	-95
1988	8	228	161	124	66	41	13	2	-18	-22
1988	9	362	304	257	187	141	68	18	-27	-32
1988	10	377	322	297	264	220	124	42	-17	-25
1988	11	127	114	146	167	167	112	58	4	0
1988	12	203	146	170	173	139	66	44	23	9
1989	1	174	114	144	167	136	79	42	5	5
1989	2	293	130	155	139	99	53	32	12	10
1989	3	190	202	200	192	169	84	31	-1	-1
1989	4	322	234	186	113	88	64	69	9	1
1989	5	551	403	301	159	87	22	3	-9	-12
1989	6	288	288	206	62	27	-1	3	-36	-67
1989	7	175	187	137	58	31	-7	-12	-135	-151
1989	8	78	117	110	102	64	4	-6	-89	-78
1989	9	90	142	184	214	190	78	10	-24	-17
1989	10	194	311	333	347	306	161	72	-5	-5
1989	11	301	324	281	253	214	128	122	24	14
1989	12	125	172	140	146	140	87	49	-12	-18
1990	1	103	213	239	303	299	217	105	10	7
1990	2	87	111	135	167	152	107	76	74	54
1990	3	109	122	149	203	227	184	94	56	48
1990	4	165	157	144	137	113	56	4	-1	0
1990	5	109	134	72	31	35	12	1	-20	-26
1990	6	118	170	128	71	71	24	6	-81	-95
1990	7	128	185	179	88	40	0	-39	-208	-171
1990	8	235	244	215	129	111	49	13	-19	-27
1990	9	525	418	387	199	130	73	42	4	0
1990	10	617	562	583	395	305	234	156	12	2
1990	11	350	402	560	517	483	379	199	2	2
1990	12	188	273	400	463	428	324	141	14	8

Year	Month	15°S, 12°E	18°S, 11°E	21°S, 13°E	24°S, 14°E	27°S, 15°E	30°S, 17°E	33°S, 17°E	36°S, 20°E	36°S, 23°E
1991	1	95	134	254	351	351	302	186	7	2
1991	2	62	114.5	187	258	271	222	137	13.5	8.5
1991	3	29	95	120	165	191	142	88	20	15
1991	4	33	100	84	90	119	73	28	-4	-5
1991	5	6	98	72	53	42	6	-1	-41	-60
1991	6	70	148	104	32	8	-2	-2	-18	-20
1991	7	61	108	81	29	20	0	-2	-64	-68
1991	8	361	368	278	160	135	62	9	-40	-58
1991	9	818	549	545	283	129	43	4	-34	-35
1991	10	718	607	751	500	345	235	151	36	31
1991	11	343	475	582	497	476	331	100	-2	0
1991	12	171	315	389	336	306	205	23	-3	0
1992	1	71	152	255	323	347	273	105	3	2
1992	2	107	297	478	427	264	108	9	-1	2
1992	3	103	222	268	263	230	135	78	24	14
1992	4	42	251	269	303	282	121	13	-31	-22
1992	5	1	171	132	155	205	63	3	-210	-223
1992	6	57	160	100	33	25	-5	-27	-197	-210
1992	7	63	181	113	62	54	1	-14	-122	-127
1992	8	458	399	276	140	118	34	27	-6	-12
1992	9	831	500	447	340	354	196	37	-17	-18
1992	10	801	602	642	392	229	94	28	6	5
1992	11	533	567	616	492	371	200	77	3	1
1992	12	367	472	690	706	542	296	40	-24	-15
1993	1	71	152	255	323	347	273	105	3	2
1993	2	80	142	236	304	288	197	80	5	4
1993	3	56	106	142	219	291	206	89	21	17
1993	4	131	240	211	183	184	95	55	4	-2
1993	5	75	203	213	176	130	31	4	-59	-72
1993	6	10	68	14	-13	16	-6	2	-52	-72
1993	7	6	96	42	9	2	-29	-38	-85	-105
1993	8	210	208	94	41	56	18	13	-9	-18
1993	9	269	210	133	134	222	137	37	-3	-3
1993	10	872	723	692	503	437	261	71	5	9
1993	11	425	486	565	462	350	200	68	6	11
1993	12	360	422	515	512	440	297	120	5	2
1994	1	322	265	317	349	328	216	76	16	13
1994	2	232	212	257	280	255	181	103	62	57
1994	3	197	284	309	314	247	133	64	42	40
1994	4	230	227	126	69	82	46	26	6	1
1994	5	62	109	72	96	153	44	1	-35	-42
1994	6	45	208	133	74	60	-9	-44	-252	-253
1994	7	-20	84	32	34	64	-11	-2	-83	-97
1994	8	169	256	180	128	155	51	31	0	-1
1994	9	917	587	483	289	137	26	1	-7	-5
1994	10	874	767	663	509	420	182	67	4	3
1994	11	686	743	729	574	385	151	16	-26	-8
1994	12	361	601	628	515	378	201	69	11	19
1995	1	532	606	615	537	393	258	78	7	12
1995	2	661	489	445	380	321	211	95	24	26
1995	3	259	399	340	283	277	152	92	66	51
1995	4	9	190	157	173	212	117	76	13	4
1995	5	49	113	55	38	61	12	14	-1	-2
1995	6	-56	51	36	46	45	-10	-6	-71	-90
1995	7	20	250	202	152	145	9	-11	-182	-182
1995	8	376	447	351	229	145	28	4	-13	-11
1995	9	640	467	487	422	296	95	19	-4	0
1995	10	1035	805	740	491	264	91	16	-3	-1
1995	11	900	690	659	553	458	278	148	21	16
1995	12	697	539	529	449	267	142	128	165	142

Year	Month	15°S, 12°E	18°S, 11°E	21°S, 13°E	24°S, 14°E	27°S, 15°E	30°S, 17°E	33°S, 17°E	36°S, 20°E	36°S, 23°E
1996	1	746	506	564	556	415	266	116	20	14
1996	2	691	435	393	344	268	163	78	21	21
1996	3	382	406	346	287	277	151	63	15	9
1996	4	14	179	133	136	134	51	25	6	9
1996	5	100	205	122	106	77	13	2	-9	-9
1996	6	13	116	63	45	37	-16	-48	-235	-227
1996	7	61	209	135	79	73	0	0	-40	-46
1996	8	664	499	428	224	87	2	-10	-56	-50
1996	9	1145	756	684	439	235	54	7	-80	-52
1996	10	1372	954	905	738	518	292	149	39	29
1996	11	1357	981	906	652	501	271	114	6	4
1996	12	1026	807	850	696	555	306	130	11	10
1997	1	560	513	691	619	527	362	161	11	11
1997	2	376	455	523	474	490	340	205	28	11
1997	3	144	392	391	302	320	192	116	54	48
1997	4	14	246	170	97	124	53	34	0	1
1997	5	-68	63	8	7	29	2	7	-3	-3
1997	6	-17	101	32	8	15	-2	-10	-75	-76
1997	7	-41	87	17	-6	21	-9	14	-9	-18
1997	8	225	198	105	63	99	31	14	-29	-24
1997	9	695	445	339	211	196	80	46	9	8
1997	10	511	474	491	339	290	144	92	17	13
1997	11	444	542	558	388	296	143	68	14	11
1997	12	367	597	643	520	395	205	71	3	4
1998	1	357	517	620	531	427	249	114	-1	0
1998	2	183	493	489	426	375	218	148	69	52
1998	3	51	406	403	353	342	198	108	16	9
1998	4	-108	51	20	36	105	24	17	-2	-2
1998	5	-189	-2	-6	6	40	-1	-4	-38	-39
1998	6	-473	-94	-59	0	54	0	-8	-127	-174
1998	7	-12	202	38	14	48	-2	6	-53	-76
1998	8	142	303	65	11	60	8	19	-20	-29
1998	9	613	745	488	271	238	95	57	-9	-11
1998	10	989	967	719	435	274	110	85	4	-1
1998	11	506	845	637	455	373	198	128	1	3
1998	12	422	582	538	503	338	183	128	34	28
1999	1	199	473	401	373	372	237	181	36	31
1999	2	40	296	274	271	274	164	190	72	51
1999	3	24	266	128	108	186	105	120	32	28
1999	4	-67	137	32	26	65	7	47	16	5
1999	5	-5	165	35	23	46	4	14	-7	-17
1999	6	-84	44	-22	-40	-33	-81	-9	-48	-75
1999	7	-83	83	2	-19	4	-26	-10	-57	-53
1999	8	73	248	71	7	13	-10	-11	-88	-97
1999	9	474	591	308	121	113	29	48	-17	-16
1999	10	731	712	432	265	239	107	114	18	10
1999	11	697	821	693	530	429	212	108	3	3
1999	12	411	480	490	392	278	128	102	48	39
2000	1	320	476	451	309	225	116	156	61	47
2000	2	287	537	600	552	468	301	221	44	28
2000	3	97	427	344	294	322	204	265	118	78
2000	4	-55	158	86	83	108	22	56	31	16
2000	5	-101	76	12	10	37	-3	0	-5	-13
2000	6	-218	15	-38	-62	-33	-67	-34	-139	-137
2000	7	-95	48	-11	-48	-11	-37	-4	-74	-98
2000	8	53	197	47	22	81	9	11	-47	-50
2000	9	624	710	455	229	184	33	19	-74	-65
2000	10	686	812	680	486	389	163	116	26	16
2000	11	817	826	739	478	285	132	77	9	9
2000	12	782	753	769	694	531	312	145	-7	-13

Overall Mean Monthly Coastal Values

Month	15°S, 12°E	18°S, 11°E	21°S, 13°E	24°S, 14°E	27°S, 15°E	30°S, 17°E	33°S, 17°E	36°S, 20°E	36°S, 23°E
1	222.4	271.4	329.6	385.1	349.2	223.1	100.2	8.2	5.8
2	178.7	232.6	276.1	315.1	285.3	175.8	102.6	27.6	20.1
3	118.3	228.1	245.3	278.4	263.1	151.2	85.6	25.5	18.1
4	83.7	192.1	182.1	182.4	161.5	69.0	32.8	1.4	-1.9
5	94.9	171.4	137.7	108.9	87.7	20.7	2.4	-39.0	-43.1
6	31.6	141.1	106.8	60.8	44.7	-2.4	-10.7	-89.2	-96.9
7	74.4	175.6	130.2	76.6	59.3	2.9	-5.8	-77.3	-82.5
8	208.6	247.0	184.2	129.7	104.3	30.1	7.6	-37.1	-40.3
9	455.0	393.3	337.0	251.0	189.0	72.7	21.2	-25.7	-23.2
10	566.7	523.1	505.2	417.6	319.8	163.3	76.7	7.3	4.3
11	443.4	478.7	503.5	473.7	381.9	210.4	89.7	4.3	4.7
12	329.2	383.1	433.9	454.4	364.1	201.9	80.4	8.7	6.0

APPENDIX II

AROMK1 PROGRAM DATA OUTPUT DESCRIPTION

AROMK1 DATA OUTPUT DESCRIPTION

The upwelling index presented in this report is computed with the standard Aromk1 program developed at the Pacific Fisheries Environmental Laboratory by Andrew Bakun, Arthur Stroud, David Husby and Craig Nelson (Bakun, 1973, Nelson, 1977). Aromk1 alternative inputs/outputs include, monthly data from monthly mean pressure fields (used in this report), six-hourly data from six-hourly pressure fields (both available from http://www.pfeg.noaa.gov), and monthly mean data calculated from six-hourly FNMOC pressure fields. The Aromk output header and a few lines of sample output follow.

NOAA/NMFS/SWFSC
Pacific Fisheries Environmental Laboratory
Pacific Grove, California 93950-2097

Transport Indices Computed From FNMOC Atmospheric Pressure at Mean Sea Level Global Analysis Fields (73x144 before and 181x360 after 11/1996)

Columns Description Dates: 1981010100 through 1996113018

1 - 4	Year
5 - 6	Month (mm=01 => January)
7 - 8	Day of Month (dd=01 => 1st)
9 – 10	Hour of Day (hh=00 => midnight Universal Time) or Number of Fields in daily or longer Mean product
11 – 15	Latitude (hundredths of degrees, North > 0, South <0
16 – 21	Longitude (hundredths of degrees, East > 0, West < 0
22 – 26	Atmospheric Pressure at Mean Sea Level (value +10,000)/10 => mb)
27 – 31	Wind Velocity, Northward > 0 (decimeters/sec)
32 – 36	Wind Velocity, Eastward > 0 (decimeters/sec)
37 – 41	Wind Stress, Northward > 0 (value x 1.0E-3 => dynes/cm**2)
42 – 46	Wind Stress, Eastward > 0 (value x 1.0E-3 => dynes/cm**2)
47 – 51	Wind Stress CURL (value x 1.0E-10 => dynes/cm**2/cm)
52 – 56	Wind Speed Cubed ((m/sec)**3)
57 – 61	Ekman Transport, Northward > 0 (value x 10 => metric-tons/sec/km)
62 – 66	Ekman Transport, Eastward > 0 (value x 10 => metric-tons/sec/km)
67 – 71	Offshore Ekman Transport or Upwelling Index (metric-tons/sec/100 meters of coast)
72 – 76	Offshore Direction along which Upwelling Index is resolved (degrees true)
77 – 81	Upward Vertical Velocity into Ekman Layer (mm/day excluding Coastal Divergence)
82 – 86	Sverdrup Transport, Northward > 0 (value x 100 => metric-tons/sec/km)

** The value 0.0026 was used as Drag Coefficient in the stress computations.

1981010124-1500	1000	130	40	-17	347	-138	-99	143	-37	-92	78	286	-247	45
1981020112-1500	1000	122	39	-20	320	-162	-53	131	-43	-85	70	286	-142	24
1981030124-1500	1000	127	34	-11	251	-74	-75	93	-20	-67	59	286	-182	34
1981040120-1500	1000	125	47	-24	472	-242	-127	248	-64	-125	103	286	-324	58
1981050124-1500	1000	136	54	-20	582	-228	-165	312	-60	-155	132	286	-409	75
1981060120-1500	1000	159	45	-34	493	-372	-282	319	-99	-131	99	286	-697	128
1981070124-1500	1000	169	48	-18	503	-185	-188	258	-49	-134	115	286	-456	85

RECENT TECHNICAL MEMORANDUMS

Copies of this and other NOAA Technical Memorandums are available from the National Technical Information Service, 5285 Port Royal Road, Springfield, VA 22167. Paper copies vary in price. Microfiche copies cost $9.00. Recent issues of NOAA Technical Memorandums from the NMFS Southwest Fisheries Science Center are listed below:

NOAA-TM-NMFS-SWFSC-333 Ichthyoplankton and station data for Manta (surface) tows taken on California Cooperative Oceanic Fisheries Investigations Survey Cruises in 1997.
D.A. AMBROSE, R.L. CHARTER, H.G. MOSER
(May 2002)

334 Ichthyoplankton and station data for Manta (surface) tows taken on California Cooperative Oceanic Fisheries Investigations Survey Cruises in 1998.
D.A. AMBROSE, R.L. CHARTER, H.G. MOSER
(May 2002)

335 Ichthyoplankton and station data for Manta (surface) tows taken on California Cooperative Oceanic Fisheries Investigations Survey Cruises in 1999.
D.A. AMBROSE, R.L. CHARTER, H.G. MOSER
(May 2002)

336 Ichthyoplankton and station data for Manta (surface) tows taken on California Cooperative Oceanic Fisheries Investigations Survey Cruises in 2000.
W. WATSON, R.L. CHARTER, H.G. MOSER
(May 2002)

337 Ichthyoplankton and station data for surface (Manta) and oblique (Bongo) plankton tows taken during a survey in the eastern tropical Pacific ocean July 30-December 9, 1998.
D.A. AMBROSE, R.L. CHARTER, H.G. MOSER, S.R. CHARTER, and W. WATSON
(June 2002)

338 Ichthyoplankton and station data for surface (Manta) and oblique (Bongo) plankton tows taken during a survey in the eastern tropical Pacific ocean July 28-December 9, 1999.
W. WATSON, E.M. SANDKNOP, S.R. CHARTER, D.A. AMBROSE, R.L. CHARTER, and H.G. MOSER
(June 2002)

339 Report of ecosystem studies conducted during the 1997 Vaquita abundance survey on the research vessel David Starr Jordan.
V.A. PHILBRICK, P.C. FIEDLER, and S.B. REILLY
(June 2002)

340 The Hawaiian Monk Seal in the Northwestern Hawaiian Islands, 2000.
Compiled and edited by: T.C. JOHANOS and J.D. BAKER
(August 2002)

341 An operational model to evaluate assessment and management procedures for the North Pacific swordfish fishery.
M. LABELLE
(August 2002)

342 Ichthyoplankton and station data for surface (Manta) and oblique (Bongo) plankton tows taken during a survey in the eastern tropical Pacific ocean July 28-December 9, 2000.
D.A. AMBROSE, R.L. CHARTER, H.G. MOSER, B.S. MACCALL, and W. WATSON
(August 2002)